Eidgenössische Technische Hochschule Zürich
Swiss Federal Institute of Technology Zurich

WuLoRa: Energy-Efficient IoT Sensor Node

Semester Thesis

Akos Pasztor

pasztora@student.ethz.ch

Integrated Systems Laboratory
Department of Information Technology and Electrical Engineering
ETH Zürich

Advisor(s):
Dr. Michele Magno

Professor:
Prof. Dr. Luca Benini

June 19, 2017

Abstract

Computational performance has been steadily increasing in embedded systems for the last decades, which has led to emerging number of installed Internet-of-Things (IoT) devices and applications. Although hardware technology has been developing in a steep manner, battery technology has been stagnating. Therefore, low-power system design has become the most important development aspect of battery-powered embedded systems. IoT devices capable of wireless communication have to balance between network latency and battery life. One method for achieving low energy consumption is to implement heavy duty cycling of the radio module. However, putting the radio in sleep mode for long intervals greatly affects the communication latency of the node. High latency is unacceptable in safety-critical systems. In order to overcome this issue, a new, emerging technology is utilized. This state-of-the-art technology incorporates the use of an always-on wake-up radio alongside with a long-range radio transceiver. The goal of this project is do develop a new, state-of-the-art, LoRa-enabled IoT platform with a nanowatt wake-up radio; where network latency is minimized without sacrificing battery life.

Acknowledgements

I would like to express my sincere gratitude to my supervisor, Dr. Michele Magno for the continuous support of my semester project. Beside my advisors, I would like to thank the Integrated Systems Laboratory for providing me a personal workplace with access to laboratories and equipments. My sincere thank goes to Prof. Dr. Luca Benini, without whom this project would not have been possible.

Contents

List of Figures

List of Tables

Abbreviations

ADC	Analog-to-Digital Converter
ASIC	Application-Specific Integrated Circuit
FRAM	Ferroelectric RAM
FSK	Frequency-Shift Keying
GPIO	General Purpose Input/Output
IMU	Inertial Measurement Unit
IC	Integrated Circuit
IO	Input/Output
IoT	Internet of Things
IT	Interrupt
LPM	Low Power Mode
LPWAN	Low Power Wide Area Network
MCU	Microcontroller Unit
OOK	On-Off Keying
PCB	Printed Circuit Board
RAM	Random Access Memory
RTC	Real Time Clock
SPI	Serial Peripheral Interface
UART	Universal Asynchronous Receiver/Transmitter
ULP	Ultra-Low Power
WDT	Watchdog Timer
WuB	Wake-Up Beacon
WuR	Wake-Up Radio

Chapter 1

Introduction

The number of Internet-of-Things (IoT) devices has been greatly emerging during recent years. In 2015, the number of installed IoT devices were 15.4 billion. This number grew to 17.68 billion in 2016. Analysts predict that the number of deployed IoT devices will be doubled by 2020 and it will reach 75 billion by 2025 [1]. This significant growth led to increasing numbers of technologies and hardware components that are specifically developed for IoT applications. As these new technologies become not just widely available but also become affordable, it is not surprising that the number of IoT applications grow in such great manner.

In the industry of embedded systems, computational power has been steadily increasing for the last decades according to Moore's law [2]. As technology advances, new processors and chips become not only more powerful but also affordable. On the other hand, battery technology – unfortunately– has been stagnating, and despite some small breakthroughs, even the newest battery technologies cannot keep up with the steep growth of processor performance. Despite the fact that embedded system developers spend significant amount of time to optimize and achieve the best battery performance, battery-powered applications still face the problem of desperately low battery life. Conclusively, the area of low-power system design and ultra-low power technologies have become extremely demanding in battery-powered embedded systems and IoT applications.

1.1 Motivation

The bottleneck of the battery-powered wireless IoT applications is usually the communication. Regardless of protocol, wireless communication is the most energy-demanding subsystem of an IoT end-node. Even during radio listening, the energy consumption of the system is at least ten orders of magnitude higher

compared to when the radio module is completely switched off. Henceforth during development, engineers have to find balance between power consumption and network latency. The power consumption can only be decreased – that is, node battery life is extended – in exchange of increased network latency. However, increased latency can be potentially dangerous in safety-critical applications. The goal of this project is do develop a new, state-of-the-art IoT platform where network latency is minimized without sacrificing battery life.

1.2 Contribution

This project presents an efficient, low-latency, ultra-low power, LoRa-enabled IoT end-node, called WuLoRa. A preliminary prototype was made last year with LoRa-enabled radio transceiver, ultra-low power wake-up circuit, energy harvesting and sensor subsystems. The purpose of this thesis is to further improve the WuLoRa platform. The following list summarizes the contribution and work that has been made.

- Evaluate the preliminary prototype.
- Revive and initialize all subsystems and components.
- Test out each subsystem for different scenarios thoroughfully.
- Correct the hardware-issues, improve the schematics of the system.
- Create new prototype revision: redesign hardware and printed circuit board.
- Manufacture small batch of new prototype.
- Perform extensive power analysis of system in different scenarios, focusing on ultra-low power performance.

1.3 Scope of Work

In Chapter 2, the project background, including used technologies and components is described extensively. The system design is described in Chapter 3. The hardware evaluation alongside with an extensive power analysis is presented in Chapter 4. Chapter 5 contains the conclusion and project outlook.

Chapter 2

Background

In this chapter, the background of the system is presented alongside with the used state-of-the-art technologies and main components. For the Wake-up LoRa IoT node prototype, off-the-shelf components are used. The chosen major components are the MSP430 with FRAM as the main microcontroller, the RFM95W LoRa-enabled transceiver as the main radio module, the BQ25570 energy harvester and power management IC, the PIC12LF1552 nanowatt microcontroller for the wake-up circuit and various sensors to measure environmental values.

2.1 LoRa - Long Range Radio

LoRa is a proprietary modulation technique invented and owned by Semtech Corporation. It stands for Long Range and is specifically built and enhanced for IoT applications. The LoRa technology offers long range and low power wireless communication with secure data transmission. It can be used in both public and private networks to provide better coverage compared existing cellular network solutions.

LoRa itself refers only to the physical/link layer technology. The modulation used in LoRa is based on spread spectrum techniques, including a modified chirp spread spectrum technique with integrated forward error correction. High receiver sensitivity is achieved due to the ability of the modem to filter and lock on to the constant chirp preamble of the LoRa signal.

Furthermore, LoRa uses the entire channel bandwidth to transmit signals, making it robust to channel noise and insensitive to frequency offsets caused by imprecise crystals and oscillators.

On the top of LoRa, several networking protocols and topologies can be utilized for IoT. The most commonly used networking protocol built upon LoRa

Wireless	Frequency	Range	Data Rate	Power
LoRa	868MHz	15km	300bps	400mW
WiFi	2.4GHz/5GHz	100m	1300Mbps	1W
Bluetooth	2.4GHz	100m	3Mbps	1W
Bluetooth LE	2.4GHz	100m	1Mbps	10mW
ZigBee	2.4GHz	10m	250kbps	1mW
GPRS	900/1800MHz	25km	171kbps	2W
EDGE	900/1800MHz	26km	384kbps	3W
HSPA	900/2100MHz	27km	56Mbps	4W
LTE	800/1800/2600MHz	28km	1Gbps	5W

Table 2.1: Comparison of wireless technologies

is called LoRaWAN. LoRaWAN is a Low Power Wide Area Network (LPWAN) specification managed by the LoRa Alliance [3]. It defines the communication protocol and system architecture.

A LoRaWAN network incorporates servers, gateways and nodes which are connected to each other in a star-of-stars topology. The end-devices - referred as nodes - communicate with the gateways which serve a transparent bridge between nodes and a central network server. The main task of the nodes are sensing, tracking and actuating and they are often deployed to remote locations.

The LoRa nodes are transmitting data wirelessly to the LoRa gateways. The

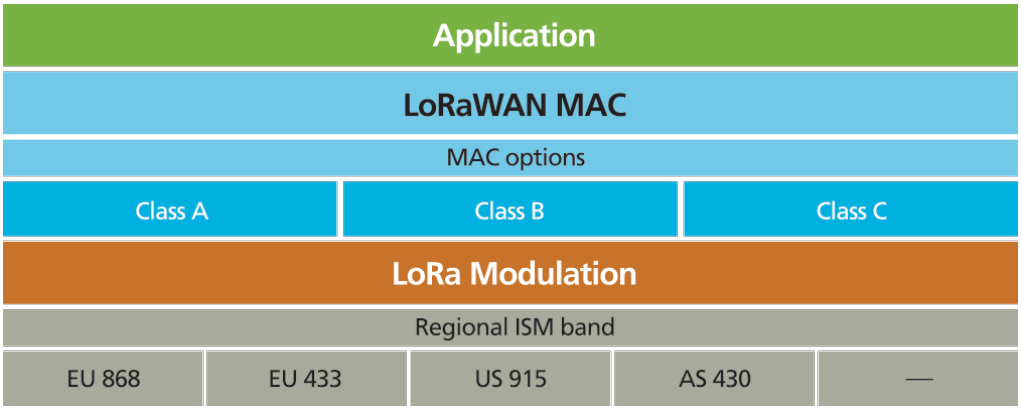

Figure 2.1: LoRa technology

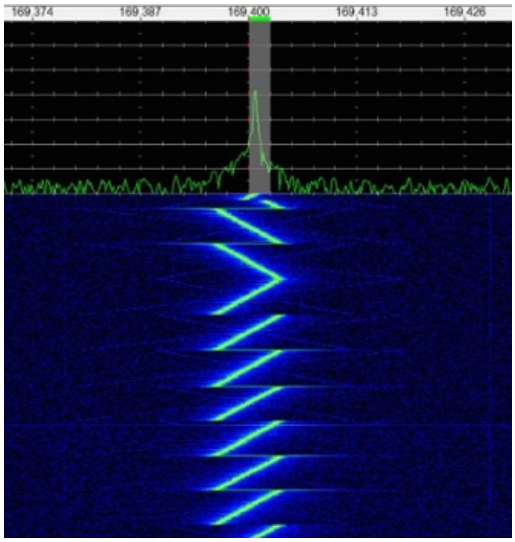

Figure 2.2: Semtech SX1276 preamble

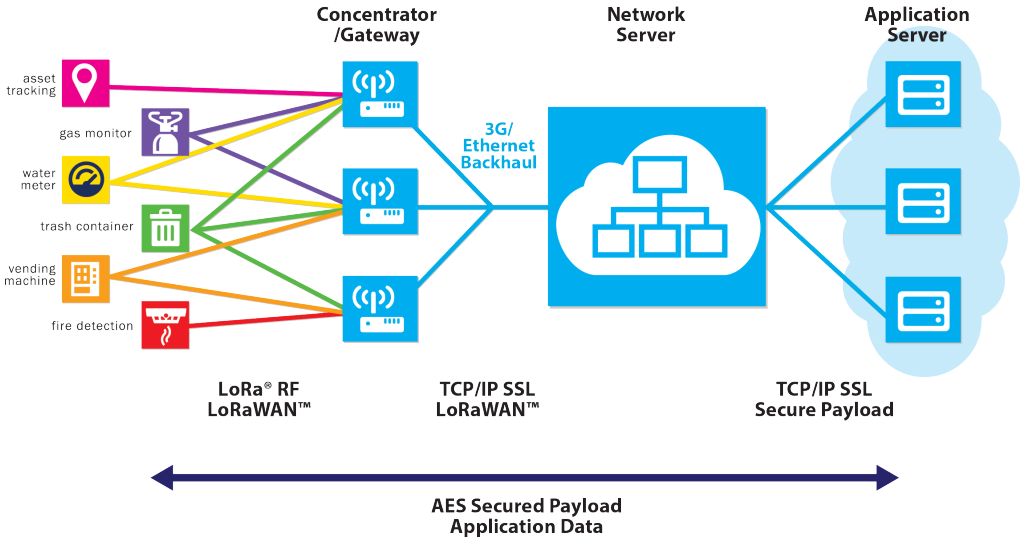

Figure 2.3: LoRa network diagram

gateways serve as base stations and they are analogous to cellular base stations, except the fact that LoRa nodes are not associated with a single gateway. Each LoRa node transmits to every gateway that is in range and every gateway forwards each packet to the network server. The gateways are connected to the network server via standard IP connections over Ethernet, Wi-Fi, cellular or other networking technology.

The network server in a LoRaWAN network embodies the intelligence: it filters out duplicate packets received from multiple gateways, acknowledges packets and performs security checks. The network server checks the packet and if required, it forwards the packet to the appropriate application server.

End nodes can operate in three different classes, depending on application requirements, latency and power consumption. Regardless of device class, all nodes are capable of bi-directional communication, however the ability how often a node can receive a packet depends on the specified device class. Class A is most suitable for battery-supplied, ultra-low power devices. The radio is in sleep mode and it is only activated when the node has to transmit a packet. While the transmission of a Class A device is not restricted, it can only receive messages in a small time window after transmission. In other words, downlink is only available after the node successfully transmits a packet to the gateway.

Class B devices have the ability to open extra receiving slots at scheduled time. The time-synchronization is implemented with a beacon that is received from a gateway. The number of additional receiving slots affect the battery life negatively. The more the device wakes up and listens for messages, the more it drains its battery.

Class C devices are always-on listeners. The radio is constantly switched on and the node has nearly always-open receive window which is only closed during transmission. Therefore, Class C devices require the most energy; that is, they have the worst battery life.

2.2 SX1276 and RFM95W

The SX1276 radio transceiver manufactured by Semtech features a LoRa modem with ultra-long range spread spectrum communication and high performance immunity [4]. Semtech invented and patented the LoRa modulation technique,

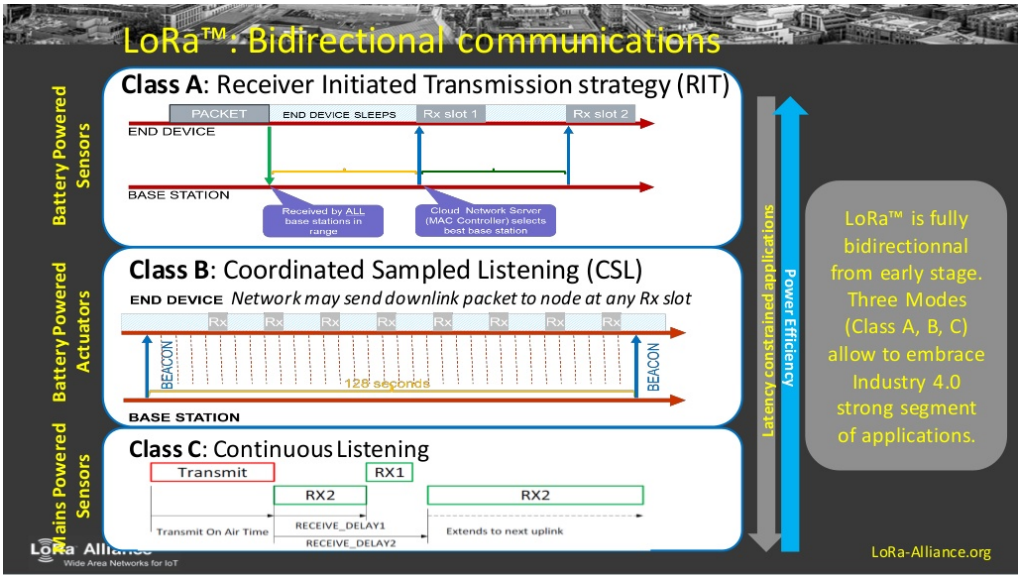

Figure 2.4: LoRa device classes

therefore currently Semtech is the only chip manufacturer that produces LoRa-enabled radio modules. The chip features not only industry-leading link budget and sensitivity, but also minimizes power dissipation and supports various low-power modes to extend battery life in IoT applications.

The key features of the SX1276 module are the followings:

- 168 dB maximum link budget
- High sensitivity: $-148dBm$
- Bullet-proof frontend: IIP3 $= -11dBm$
- Low RX current: $< 10mA$
- Register retention requires only $200nA$
- $+20dBm - 100mW$ constant RF output
- FSK, GFSK, MSK, GMSK, OOK and LoRa modulation
- Preamble detection
- Programmable bit rate up to $300kbps$
- Packet engine up to 256 bytes with CRC

The complete list of features can be found in the SX1276 datasheet [5].

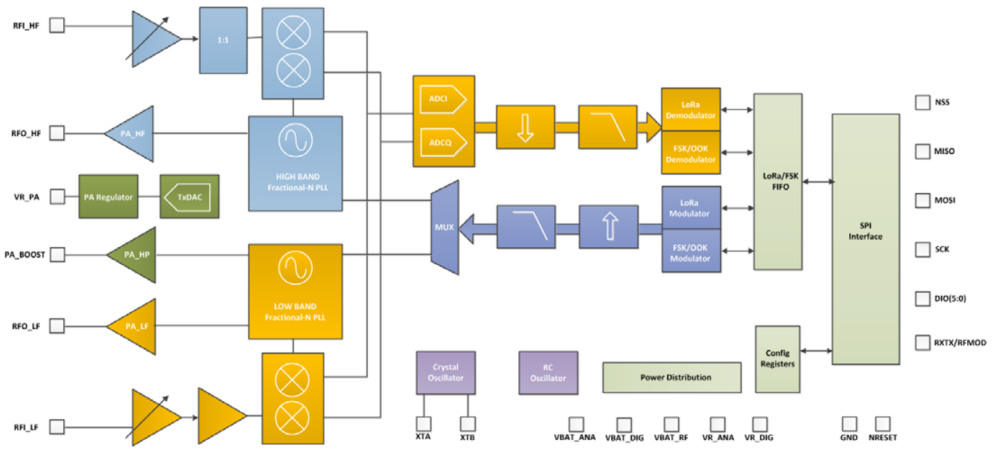

Figure 2.5: Semtech SX1276 block diagram

The RFM95W module [6] manufactured by HopeRF encapsulates the SX1276 chip alongside with the required external components, making it an easy-to-use off-the-shelf component for fast prototyping.

2.3 Wake-up Receiver

When using LoRa, the latency greatly varies between the gateway and an end-node. Since the gateways are always-on and listening, the uplink communication (from node to gateway) has minor latency, in most cases almost zero. In contrast, especially when an end-node is configured to behave as a Class A device, the node listens for downlink messages in a short time-window only after transmitting a message. Increasing the number of listening windows can reduce downlink latency however the result is a significantly increased power consumption. In applications, where low power consumption and low latency are both requirements, for example, in applications such as industrial machines, monitoring devices, medical monitoring, an alternative approach is required. A promising technology is proposed by Faycal et al., in [7]. In this work, the authors presented the idea of combining ultra-low power wake-up receivers with long-range transceivers in low-power and latency-critical applications.

A device can only receive a message when it is listening, that is, its receiver is active. However, idle listening dissipates significant power. The main principle

to reduce the power waste is to utilize a so-called wake-up radio (WuR). A WuR is an always-on circuit which is coupled with the main radio transceiver. It continuously listens for a defined message pattern and it wakes up the main radio transceiver when such message chunk is detected, thus the main radio can receive the entire incoming message.

Such wake-up radios can be divided into three main categories depending on their implementation. A *fully-passive* wake-up circuit uses the energy of the radio communication and generates an interrupt upon detection. This circuit does not consume any externally supplied power. However, this advantage has several trade-offs. First, it can only detect activity in the channel but it is not able to differentiate an RF signal from another. Therefore, these wake-up circuits cannot utilize addressing and cannot interpret commands embedded in the message. Lastly, it has low sensitivity (around $-25dBm$) compared to other types of wake-up circuits.

The majority of the wake-up systems are *semi-active*. Mainly, these circuits consist of a passive rectifier and an active comparator circuit. This approach provides reasonable sensitivity while maintaining low power consumption. A *fully-active* wake-up circuit use active components for both the rectifier and the comparator, thus achieving the highest sensitivity. On the other hand, fully active wake-up circuits have significant power dissipation, usually in the magnitude of milliwatts, compared to the previous approaches.

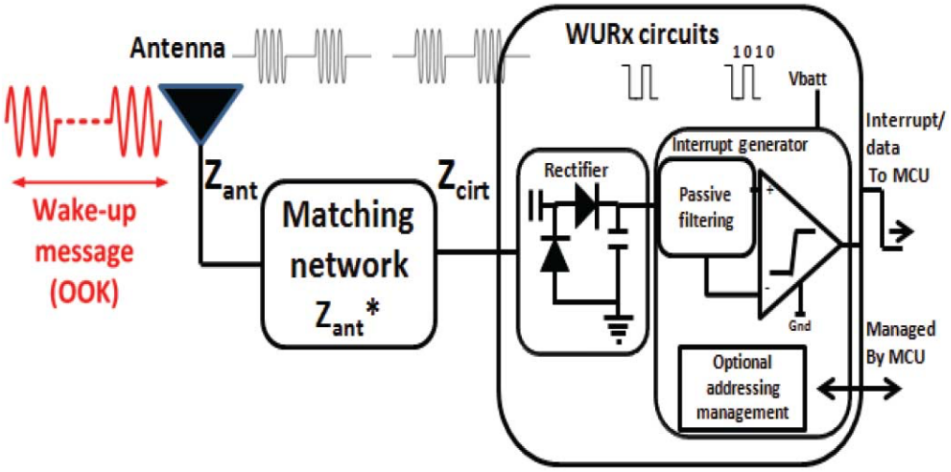

Figure 2.6: Block diagram of the wake-up receiver

In [8], a semi-active, nanowatt wake-up receiver system is presented by M. Magno et al. The wake-up circuit consists of a passive, single-stage rectifier combined with an ultra-low offset comparator and a passive interrupt generator. It is designed for demodulating OOK (On-Off Keying) wake-up signals to maintain simple circuitry thus low power consumption. Additionally, the circuit can be completed with addressing feature to reduce false-positive wake-ups. This can be implemented with an ultra-low power microcontroller or an application-specific integrated circuit (ASIC). In this work, the PIC12LF1552 ultra-low power MCU is used for addressing realization. By using only one active component, this system has extremely low power consumption while it can achieve $-55dBm$ sensitivity.

2.4 PIC12LF1552

As proposed in [8], an ultra-low power microcontroller is used for implementing addressing in the wake-up circuit and for controlling the power subsystem and waking up the main microcontroller when there is an incoming message. The PIC12LF1552 is a nanowatt-consumption, 8-bit microcontroller from Microchip [9]. It has only 8 pins and comes in various packages[1], thus the most appropriate package can be selected for the required design. The major features of the microcontroller are:

- Operating voltage range: $1.8V$ to $3.6V$
- $16MHz$ and $31kHz$ low-power internal oscillators
- Power-on reset (POR), Power-up timer (PWRT)
- Low-power brown-out reset (LPBOR), extended watchdog timer (WDT)
- 6 I/O pins with high sink/source current ($25mA$)
- 8-bit timer/counter with programmable prescaler
- 10-bit analog-to-digital converter (ADC)
- Master Synchronous Serial Port (MSSP) with SPI and I^2C
- Standby current: $20nA$ at $1.8V$
- Watchdog current: $200nA$ at $1.8V$

[1] 8-Lead PDIP, SOIC, MSOP or UDFN packages

- Operating current: $30\mu A/MHz$ at $1.8V$

Based on its parameters, this ultra-low power microcontroller is an excellent choice for the always-on wake-up radio circuit.

2.5 TI MSP430

For controlling the system, reading measurements from sensors and operating the LoRa radio module, a suitable microcontroller has to be selected. Fundamentally, any microcontroller can fulfill these requirements, however the MSP430 microcontroller family from Texas Instruments has a significant advantage over other microcontrollers: the FRAM series of the family is equipped with Ferroelectric RAM (FRAM). FRAMs are similar to DRAMs in construction, however FRAMs utilize a ferroelectric layer instead of a dielectric layer to achieve non-volatility [10]. An FRAM-equipped microcontroller is capable of zero power state retention, that is, the current state of the microcontroller is retained during power loss. In other words, after performing the required tasks, the power of the microcontroller can be entirely cut to minimize power waste and maximize battery life. After wake-up, the microcontroller can continue execution right where it was before shutdown because the entire memory state is preserved.

For this project, the ultra-low power MSP430FR5969 microcontroller from TI is selected [11]. Key features of this microcontroller are the followings:

- Supply voltage range: $1.8V$ to $3.6V$
- Low-power modes:
  - Active mode: $100\mu A/MHz$
  - Standby mode (LPM3 with VLO[1]): $0.4\mu A$
  - Low power mode with RTC[2] switched on (LPM3.5): $0.25\mu A$
  - Shutdown mode (LPM4.5): $20nA$
- 64 kbyte of FRAM
- 12-bit ADC with 16 external channels

[1] VLO: Very low power, Low frequency Oscillator
[2] RTC: Real Time Clock

- Edge-selectable wake-up from LPM modes on all ports
- Enhanced serial communication with UART, SPI and I^2C support
- Fixed frequency DCO[1] with 10 selectable frequencies
- Low-power, low-frequency internal clock source (VLO)

By choosing this microcontroller as the main processor of the system fulfills the requirements of low power consumption and computing capacity for operating the main radio module and sensor measurements.

2.6 Equipment and Tools

The following list summarizes the tools and software that have been used for development:

- Keysight MSOX2024A mixed signal oscilloscope
- RocketLogger platform[2] for logging and measuring current and energy consumption [12]
- TI MSP-EXP430FR5969 Launchpad for programming and debugging
- Microchip PICkit3 programming and debugging tool
- Altium Designer
- Texas Instruments Code Composer Studio (TI CCS)
- Microchip MPLAB X IDE
- MATLAB for measurement evaluation
- Git[3] version control system to track the progress and to provide a safety net throughout the work

[1] DCO: Digitally Controlled Oscillator
[2] RocketLogger - `https://rocketlogger.ethz.ch`
[3] Git - `https://git-scm.com`

Chapter 3

System Design

An energy-efficient IoT end-node for energy harvesting and short-long range communication was previously proposed by M. Magno et al., presented in [13]. The proposed platform comprises four subsystems:

- An always-on block with an ultra-low power microcontroller and a wake-up receiver
- Energy harvesting and power subsystem
- Sensor block with various sensors to measure ambient and environmental characteristics
- Main microcontroller and a LoRa compatible, long-range transceiver module

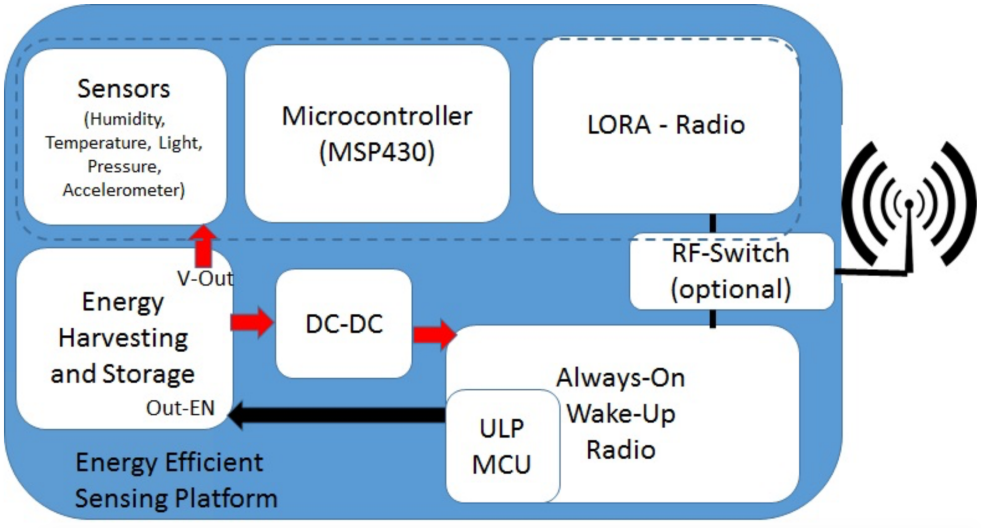

Figure 3.1: Block diagram of WuLoRa system

3.1 Always-On Subsystem

The always-on block features a wake-up receiver unit presented in [8] with a PIC12LF1552 ultra-low power microcontroller. This WUR utilizes a semi-active wake-up circuit using OOK modulation with addressing capability and it has the sensitivity of $-55dBm$ while consuming only $1\mu W$. This subsystem also controls - with the help of the nanowatt MCU - the energy harvesting block and wakes up other subsystems when it is needed.

The PIC12LF1552 microcontroller has only 8 pins. Two dedicated pins are supply pins (power and ground) and the rest six are configurable GPIO pins. These pins are also shared between the microcontroller periphery and the MCU programming interface.

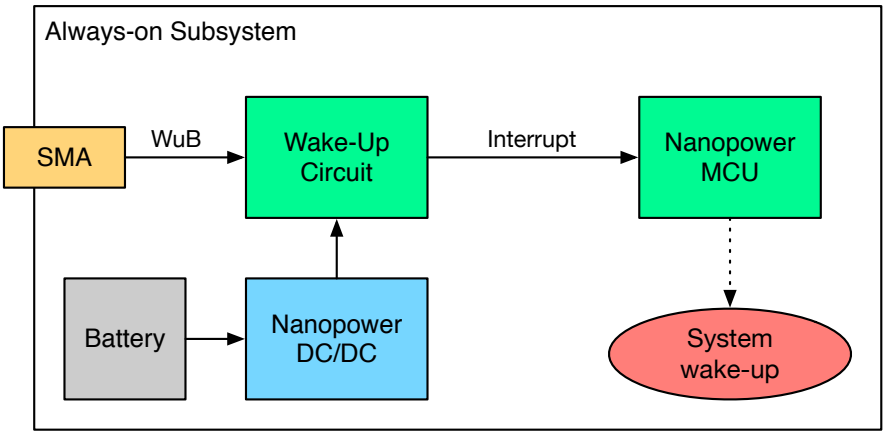

Figure 3.2: Always-on subsystem

3.2 Energy Harvesting and Power Subsystem

The platform harvests solar energy from the environment. This energy is used to provide power to other subsystems and to charge the battery. The platform utilizes the state-of-the-art BQ25570 energy harvesting chip from TI [14]. It provides 90% conversion efficiency and has a very low start-up voltage which makes the chip sufficient even for indoor applications. The harvester chip is not only capable of charging a connected battery but also incorporates a configurable buck converter, thus the rest of the platform can be powered directly without

implementing any additional power supply circuit. Finally, the chip and its submodules can be individually enabled or disabled via its dedicated pins. The Enable pin is connected to the always-on subsystem, thus the whole platform can be shut down or waken up depending on application needs and to minimize power dissipation.

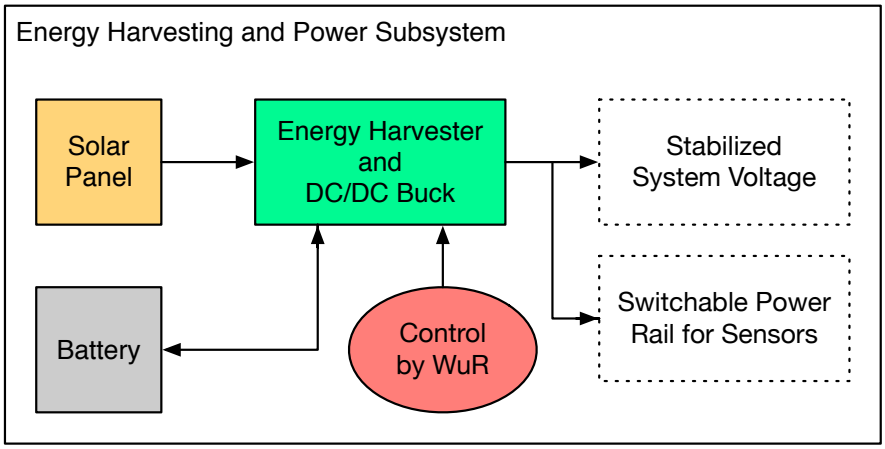

Figure 3.3: Energy harvesting and power subsystem

The sensors and the main radio module have a separate, switchable power rail. By implementing a software-controllable switching mechanism, for instance with a low $R_{DS_{(ON)}}$ power-MOSFET to minimize loss, the system can be further optimized for low power consumption. The sensors and the radio can be completely switched off when they are not needed, thus minimizing IDLE current.

In order to measure the energy consumption of the system precisely and estimate the state-of-charge (SoC) of the battery, the STC3115 gas gauge IC is used from ST Microelectronics. This small chip is suitable for portable applications for battery monitoring. It incorporates current-sensing, Coulomb counting and accurate measurement of battery voltage, thus the actual battery state-of-charge can be precisely estimated [15].

3.3 Sensor Block

The sensor block consists of numerous sensors that provides various possibilities to measure ambient and environmental values. The platform incorporates tem-

perature, humidity, light and air-pressure sensors and an Inertial Measurement Unit (IMU). The sensors are chosen as to minimize power consumption while maintaining great measurement precision.

Sensor type	**Chip**	**Power (meas.)**	**Power (idle)**
Light	ISL29023	$260\mu W$	$1\mu W$
Gas gauge	STC3115	$270\mu W$	$3\mu W$
Infrared Thermopile	TMP006	$720\mu W$	$3\mu W$
Temperature & Humidity	SHT21	$1mW$	$1.2\mu W$
Barometric Pressure	BMP180	$2mW$	$10\mu W$
IMU	MPU-9250	$9.25mW$	$20\mu W$

Table 3.1: Sensors and their power dissipation

All the sensors are communicating via a common I2C[1] interface. This design reduces the required wiring to the main microcontroller, furthermore the required design space on the PCB layout can be minimized.

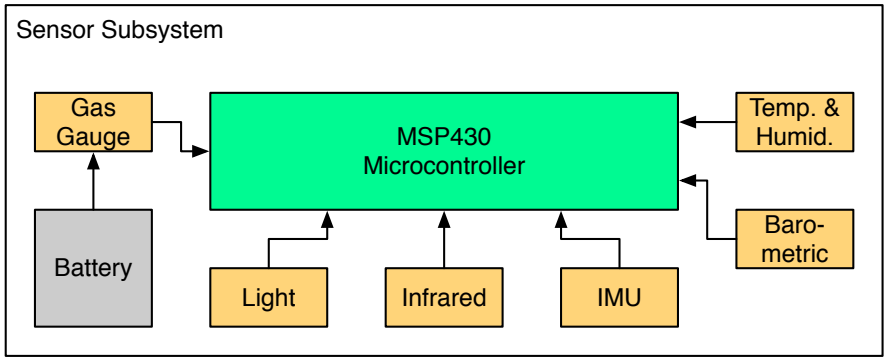

Figure 3.4: Sensor block

3.4 Microcontroller and Radio Block

The platform is driven by an ultra-low power TI MSP430FR5969 microcontroller. The sensors are connected to the MCU via a common I2C interface. The main

[1] I²C: Inter-Integrated Circuit - `https://en.wikipedia.org/wiki/I2C`

radio of the sensor node is a SX1276 low-power, long-range transceiver unit which is capable of the LoRa modulation. The radio chip is connected to the microcontroller via the SPI[1] interface.

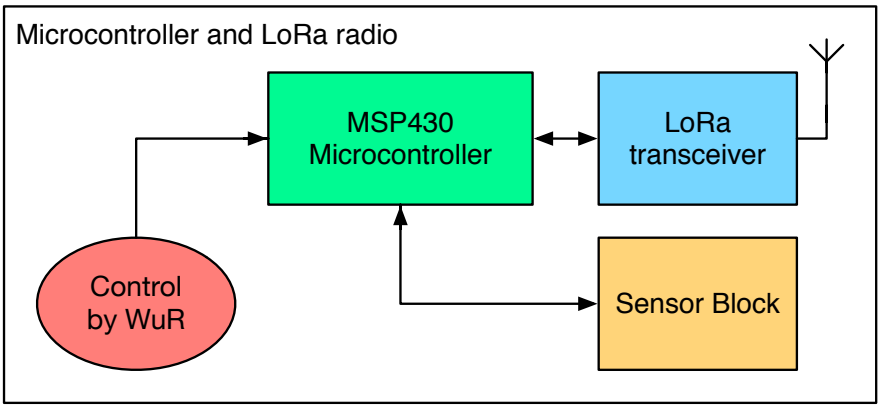

Figure 3.5: Microcontroller and Radio block

The MCU is responsible for polling the sensors for ambient and environmental measurement data, executing power management policies and communicating with other devices via the SX1276 radio transceiver. Furthermore, the MCU is equipped with an embedded FRAM. The FRAM provides data retention even when the module is not powered, making it possible to completely cut the power from the microcontroller without losing its state. Hence, the entire main microcontroller and radio subsystem can be switched off to minimize energy consumption and maximize battery lifetime.

[1] SPI: Serial Peripheral Interface Bus - https://en.wikipedia.org/wiki/Serial_Peripheral_Interface_Bus

Chapter 4

Evaluation

In this chapter the existing prototype is extensively evaluated. The necessary hardware changes are described in the Engineering Change Order (Section 4.2). A next version of the prototype is presented in Section 4.3. The system performance and detailed power analysis are presented in Section 4.4.

4.1 Hardware Evaluation

A preliminary prototype of the proposed system [13] was designed back in October 2016. This prototype realizes a fully working system, incorporating all the subsystems presented in Chapter 3. The results of the hardware evaluation show that not all the components are working as expected, therefore a new engineering change order has been proposed and ultimately a new prototype version has been developed.

4.1.1 Power Subsystem Issues

BQ25570

The energy harvester IC works as it is supposed to, it harvests energy from the solar panel, charges the connected battery and its embedded buck converter provides stabilized voltage for the rest of the system. However, the harvester has two issues. First, the output voltage of the buck converter is only $2.31V$, although the system is designed for $3.0V$ supply voltage. Furthermore, the battery overvoltage threshold and the battery voltage thresholds within operating range values are defined incorrectly. These values, alongside with the output voltage of the buck converter can be set with external resistors connected to the harvester IC.

Secondly, the buck converter of the harvester can be disabled externally by applying appropriate voltage level to the *VOUT_EN* pin. According to the datasheet [14], the buck converter is disabled when the *VOUT_EN* pin is pulled to ground; and enabled when the pin is connected to *VSTOR* – which is the output of the built-in boost charger. Depending on the light conditions, the solar panel provides different voltages over time for the harvester, resulting in constantly changing *VSTOR* voltage levels. Furthermore, the buck-enable logic tied to the *VOUT_EN* pin inside the harvester exclusively compares the applied voltage to *VSTOR*, thus the buck cannot be reliably enabled by applying a predefined, fixed voltage to the buck-enable pin. Therefore, appropriate circuit has to be designed for properly disabling and enabling the buck converter to achieve optimal system performance and low power consumption.

TPS62733

A TPS62733 step-down converter with bypass mode for ultra-low power applications from TI [16] is used to provide the required voltage for the sensors and the LoRa radio. By using a separate buck converter, the entire subsystem that is powered from this step-down converter can be entirely switched off when it is not needed to maximize battery life. When utilizing an extra DC/DC converter, the pros and cons have to be carefully investigated. The ability to switch off the entire connected subsystem might seem appealing, however several disadvantages have to be considered, including the additional power waste resulting from the efficiency, the quiescent current when the chip is disabled, the required additional space and external components to operate the converter and more.

Despite all the advantages, the selected TPS62733 chip for the preliminary prototype has an attribute that makes it unsuitable for this application. The converter has a bypass feature which is automatically activated when the chip is disabled. In other words, when the enable pin of the buck converter is pulled to ground, the chip feeds the input voltage to the output. Therefore, when a battery is connected to the input and the chip is disabled, the battery voltage appears on the output which not only powers the connected subsystem, but also can cause damage because the voltage is not regulated in bypass mode.

In most application scenarios, the always-on subsystem wakes up the main microcontroller, the radio and the sensors. The MCU polls the sensors for mea-

surement data and performs wireless communication over the network, then the system goes back to sleep. Conclusively, the sensors are switched on while the microcontroller and the radio are also in operation. Therefore, supplying the sensors from the same power rail that supplies power to the microcontroller and the radio does not affect system performance and battery life, furthermore the cost of an additional buck converter can be saved. For the sake of simplicity and to save space on the hardware PCB, the next prototype features a single, common power rail that supplies the main microcontroller, the radio and sensor modules.

4.1.2 Sensor Subsystem Issues

MPU-9250

The MPU-9250 inertial measurement unit incorporates an accelerometer, a gyroscope and a compass to track device motion. It can communicate via SPI or I^2C with a microcontroller, however the pins used for SPI and I^2C communication are shared. Therefore, the pins need to be carefully connected to the microcontroller according to the datasheet [17]. The WuLoRa system uses a shared I^2C interface to communicate with the sensors. In the preliminary prototype, the communication lines are connected erroneously; furthermore the *nCS* pin of the sensor needs to be tied to VCC.

STC3115

In order to use the *RSTIO* pin to improve initial open-circuit voltage measurement, it needs to be connected to the microcontroller and has to be pulled to VCC with an appropriate pull-up resistor.

Secondly, the jumper system that is used for debugging purposes – and which consists of the *Batt Cons* two-pin jumper and a three-pin jumper – is impractical and redundant. Furthermore, if the *Batt Cons* jumper is shorted, and the VCC and the middle pin of the three-pin jumper is connected, there is a short-circuit between the battery and the main VCC power rail, which may damage the hardware.

4.1.3 Always-On Subsystem Issues

The PIC12LF1552 nanowatt microcontroller used in the always-on subsystem has only eight pins, which greatly limits its connectivity to other components. However, the PIC microcontroller needs to communicate with the MSP430 main MCU, but this can be done either via SPI or via I^2C. The MSP430 has only two serial interface that can be used for I^2C and SPI communications. The I^2C is used for sensor communication and the SPI interface is reserved for communicating with the radio module. Hence, the PIC uses the shared I^2C bus to communicate with the MSP430. In the scenario when the MSP430 is completely switched off but the I^2C lines are pulled up, a new source of power waste is introduced.

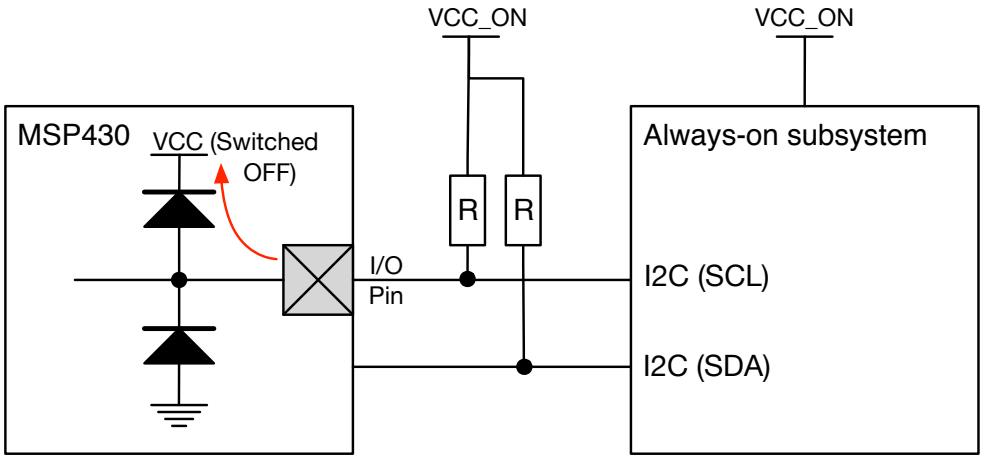

Figure 4.1: Microcontroller I/O pin protection

As demonstrated in Figure 4.1, when the microcontroller and its power rail is powered down while the I^2C lines are pulled up, voltage appears on the VCC line through the internal protection circuit of the microcontroller IO pin. This voltage can power-up components connected to the VCC line which results in unnecessary power dissipation. A solution for this problem is to pull the I^2C communication lines to the power rail of the main microcontroller, however the drawback of this solution is that the I^2C bus is only usable when the whole system is powered.

4.1.4 Miscellaneous Issues

LED values

The LED values require a few milliamperes to operate, which can be achieved by using resistors that have values in the order of a few hundred Ohms.

Pull-up resistor values

Generally, pull-up resistor values for communication lines and IO lines should be as high as possible to further minimize power dissipation. However, using weaker pull-ups can affect system performance: a line with a higher value of pull-up resistor is pulled up slower, because the time constant of the pull-up resistor and the surrounding stray capacitance increases. For instance, when an I^2C communication bus needs to operate with a higher frequency to achieve greater communication speed, high pull-up values should not be used.

4.2 Engineering Change Order

Considering the issues described in Section 4.1, alongside with overall system improvement considerations, the following engineering change order is proposed for the new prototype.

- Resistor values for the energy harvester IC are changed to properly set the output voltage of the embedded buck converter.
- Resistor values for the energy harvester IC are changed to properly set the battery overvoltage threshold value and the voltage thresholds within operating range values.
- The buck-enable circuit for the energy harvester IC is completely redesigned in order to realize proper enable and disable functionality of the embedded buck converter.
- The TPS62733 DC/DC converter which provides a separate power line for the sensors and the main radio is removed. The power rails of the main microcontroller, sensors and the radio are merged to a single power line, henceforth labelled as VCC. Sensors and their power pins alongside with the required pull-up resistors are connected to the merged power rail.

- The lines of the shared I^2C communication bus between the the sensors, the PIC and the main microcontroller are pulled to VCC.
- The I^2C lines are correctly connected to the MPU-9250 IMU.
- The *RSTIO* line of the STC3115 gas gauge IC is connected to VCC via a pull-up resistor.
- The jumper system for the STC3115 IC is replaced with a single, 3-pin header in order to decrease redundancy and prevent accidental short circuit between the battery and the VCC line.
- LED resistor values are changed to correct values.
- Additional solder bridges are added for easier hardware debugging.

4.3 New Hardware Prototype

Based on the engineering change order described in Section 4.2, a new prototype of the WuLoRa system is developed. The schematics are modified accordingly, moreover several minor design enhancements are made, including the implementation of hierarchical schematic design and proper Altium documentation. The schematics of the prototype redesign can be found in Appendix B.

The layout of the printed circuit board is also modified. The 4-layer PCB layout and board dimensions remained the same, however wiring and routing are highly optimized, and additional polygon pours are introduced on the top and bottom layers for noise resilience. Screenshots and images of the new PCB layout can be found in Appendix C. The new prototype is manufactured by Multi Circuit Boards Ltd[1] and assembled at the IIS laboratory at ETH Zürich.

4.4 Power Analysis

In this section, the results of power dissipation measurements performed in different scenarios are presented. To perform precise measurements, the RocketLogger measurement device is used [12]. The RocketLogger device is developed at ETH Zürich, and it features two current channels with high dynamic range from $4nA$ up to 500mA, four voltage channels measuring from $13\mu V$ up to $5.5V$, fast and

[1] Multi Circuit Boards Ltd. - `https://www.multi-circuit-boards.eu`

seamless range switching and more. The RocketLogger can be connected to the local network and it features a web-based interface where configuration and logging features can be adjusted, furthermore data is shown in real-time during measurement. The device is capable of logging each measurement and the data can be downloaded to the computer for further processing. The data can be processed conveniently in MATLAB with scripts provided in the RocketLogger project repository[1].

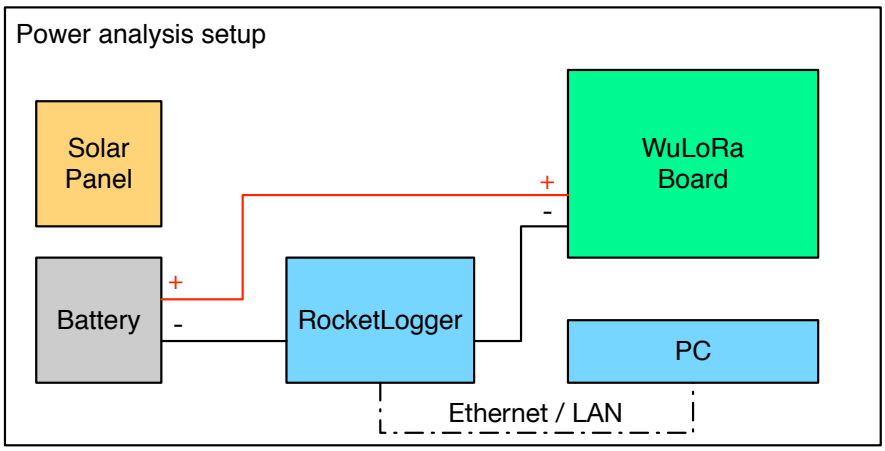

Figure 4.2: Power analysis setup

The power analysis setup is demonstrated in Figure 4.2. The RocketLogger is connected between the grounds to perform low-side current sensing. The advantage of this method is the common-mode voltage or the average voltage at the measurement inputs is near zero. This provides precise current measurement where the supply voltage of the application is prone to high voltage spikes or surges [18]. Furthermore, the RocketLogger is placed to sense current just after the battery, thus the entire power dissipation of the system can be precisely measured, including the waste during DC/DC conversion and quiescent current consumption.

The RocketLogger is configured to perform 1000 samples per second in each scenario. The following list summarizes the power analysis scenarios that have been chosen to evaluate the energy consumption of the WuLoRa.

1. Only the always-on subsystem is active, the PIC microcontroller is in sleep

[1] RocketLogger project repository - `https://git.ee.ethz.ch/sigristl/rocketlogger/`

mode.

2. Only the always-on subsystem is active, the PIC microcontroller is in active mode.
3. MSP430 is active, sensors are off, main radio is off.
4. MSP430 is active, sensors are on, main radio is off.
5. MSP430 is active and performs sensor measurement, main radio is off.
6. Main radio is on, configured in OOK mode with +10dBm transmission power. The radio sends messages periodically and it is in receive mode between transmissions.
7. Main radio is on, configured in LoRa mode and sending messages periodically. The radio is in receive mode between transmissions.
   (a) $0dBm$ TX power during transmission
   (b) $+5dBm$ TX power during transmission
   (c) $+10dBm$ TX power during transmission
   (d) $+14dBm$ TX power during transmission
   (e) $+17dBm$ TX power during transmission
   (f) $+20dBm$ TX power during transmission

4.4.1 Scenario 1-2: Always-on Subsystem

During standby mode, the entire system is shut down, except for the always-on subsystem. In this scenario, only the wake-up circuit is active, however the PIC microcontroller is in sleep mode. Figure 4.3 shows the power consumption of this scheme. The average power dissipation of the whole system is $2.091\mu W$. Summarizing the consumptions of the PIC microcontroller in sleep mode and the dissipation of the wake-up circuit based on the datasheets of the individual components, the measured average consumption confirms the calculated theoretical values.

When a wake-up beacon is received, the wake-up circuit issues an interrupt for the PIC microcontroller and it wakes up from sleep mode. When the PIC is active, the power consumption increases sightly, as shown in Figure 4.4. In active mode, the MCU runs at $1MHz$ and based on its datasheet, it drains approximately $30\mu A/MHz$. Therefore, the increased power dissipation at $3.0V$ is

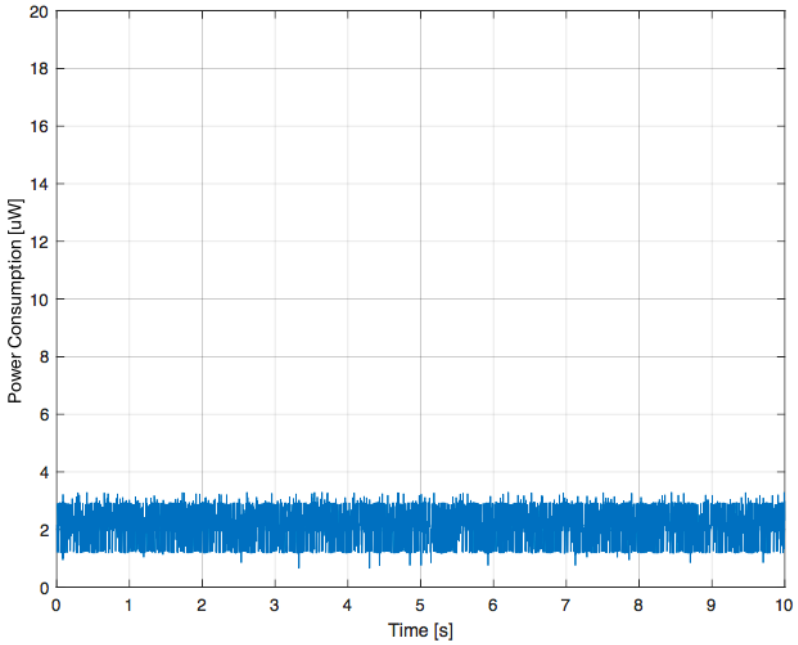

Figure 4.3: Power consumption during deep-sleep

approximately $90\mu W$, which is confirmed by the measured average consumption of the system ($93.830\mu W$).

4.4.2 Scenario 3-5: Active MCU and Sensor Measurements

As soon as the PIC receives a valid wake-up beacon, it switches on the main power circuit and the MSP430 main microcontroller. The MSP430 runs at $1MHz$ and draws approximately $100\mu A$ current per MHz, which results in a theoretical dissipation of $300\mu W$ at $3.0V$. However, due to the DC/DC loss of the power subsystem and the quiescent current of external and auxiliary components, the measured average power consumption of the overall system is significantly higher, $4.534mW$. Figure 4.5 demonstrates this scenario.

The main microcontroller performs sensor measurements during its active state. The sensors are switched on and polled by the MCU via the I^2C communication interface. During measurements, the sensors draw additional current to perform their measurements and to communicate with the microcontroller. Figure 4.6 illustrates this scenario: after a few seconds, the sensors are switched

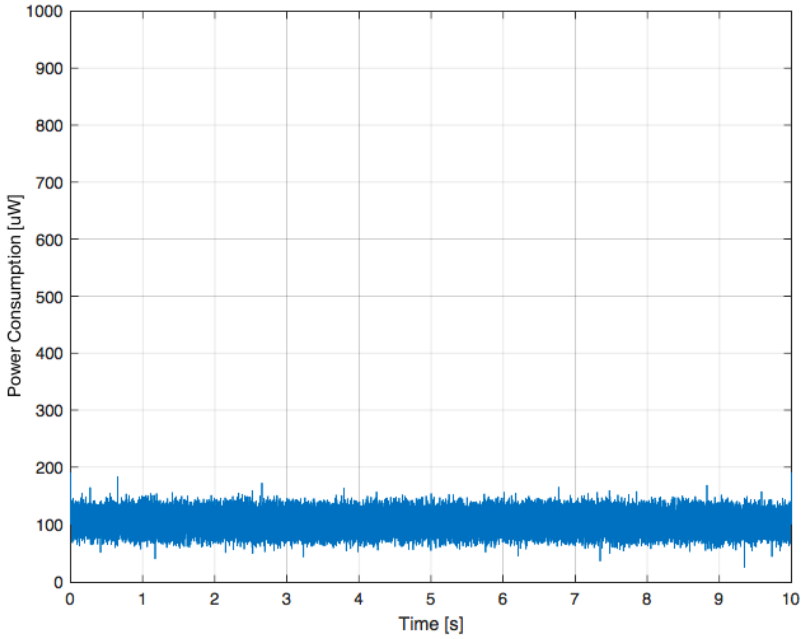

Figure 4.4: Power consumption when the PIC MCU is active

on and they perform the measurements. The average power drain of the system during measurements is approximately $10.671mW$.

4.4.3 Scenario 6: Radio in OOK Mode

In the following scenarios, the performance and power consumption of the main radio is tested. In all scenarios, the task to be executed remains the same: the radio is switched on and set to receive mode. After a few seconds, the radio switches to transmission mode and transmits a short message. After transmission, the radio is switched back to receiver mode and it continues listening. The performance and power consumption of the radio module is tested in OOK and LoRa modes, with different transmission power settings.

Figure 4.7 illustrates the power consumption of the system when the radio is configured in OOK mode. During transmission, the transmission power is set to $+10dBm$. The average power consumption while listening is $14.8mW$ and $265mW$ during message transmission.

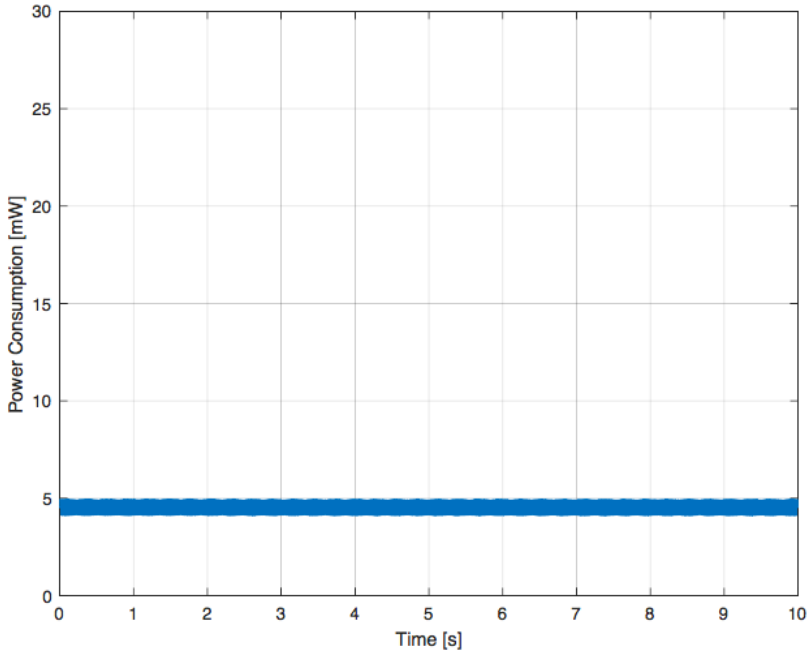

Figure 4.5: Power consumption when the main MCU is active

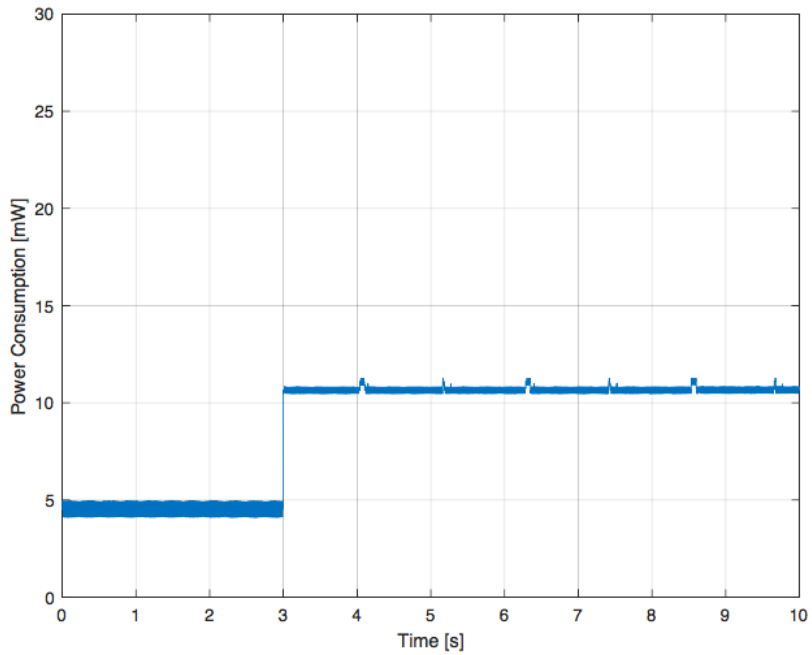

Figure 4.6: Power consumption when the MCU performs sensor measurements

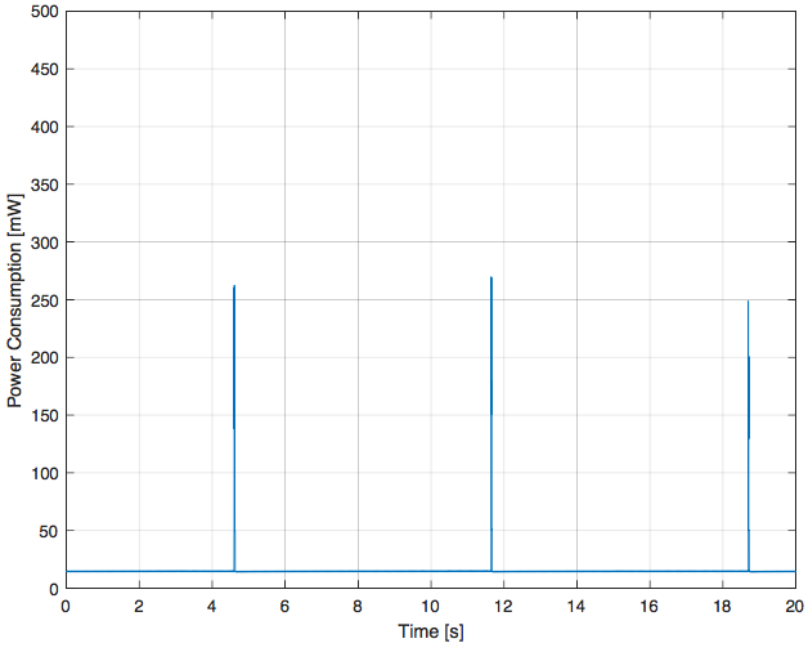

Figure 4.7: Power drain when the radio is on (OOK mode, $+10dBm$ TX power)

4.4.4 Scenario 7: Radio in LoRa Mode

Extensive power analysis is performed in order to obtain a complete picture about the power consumption of the radio configured in LoRa mode. The radio is configured with the parameters listed below. During the analysis, the transmission power of the radio module is changed from $0dBm$ to $+20dBm$ (maximum power).

- Bandwidth: 125kHz
- Data rate: 12 (4096 chips)
- Coding rate: 4/5
- Preamble length: 4 symbols
- CRC: disabled
- Intra-packet frequency hopping: disabled

The commencing figures (Figure 4.8 - 4.13 demonstrate the results of the power analysis in different transmission power configurations.

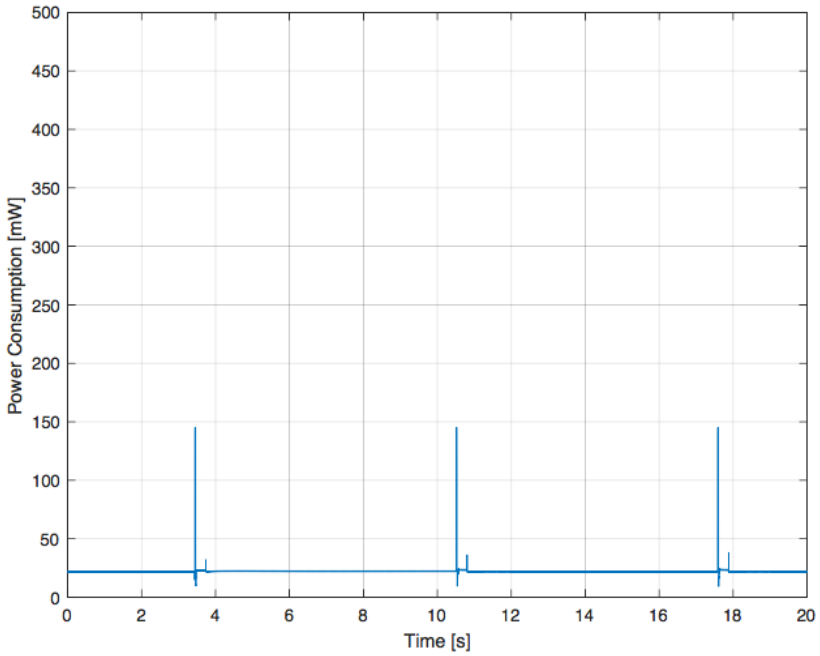

Figure 4.8: Power drain when the radio is on (LoRa mode, $0dBm$ TX power)

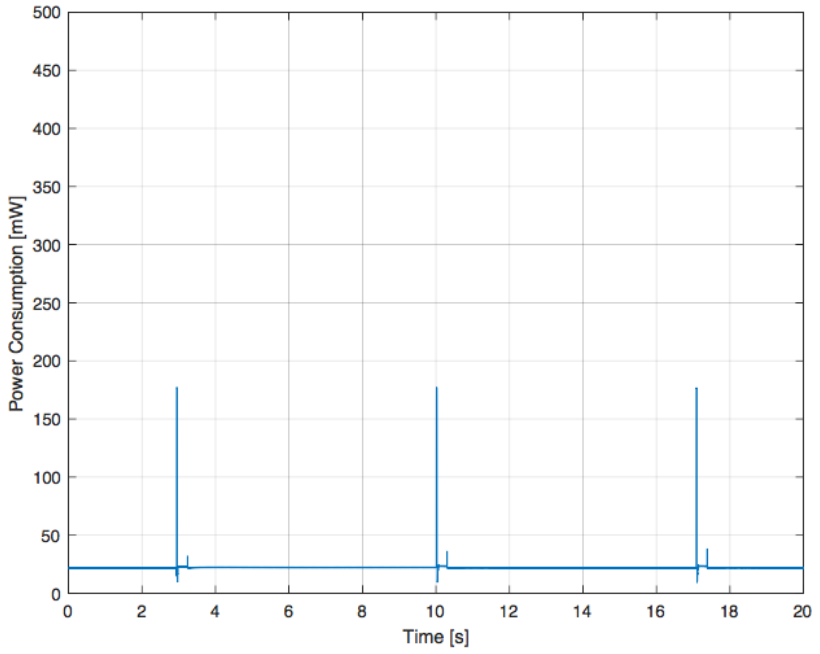

Figure 4.9: Power drain when the radio is on (LoRa mode, $+5dBm$ TX power)

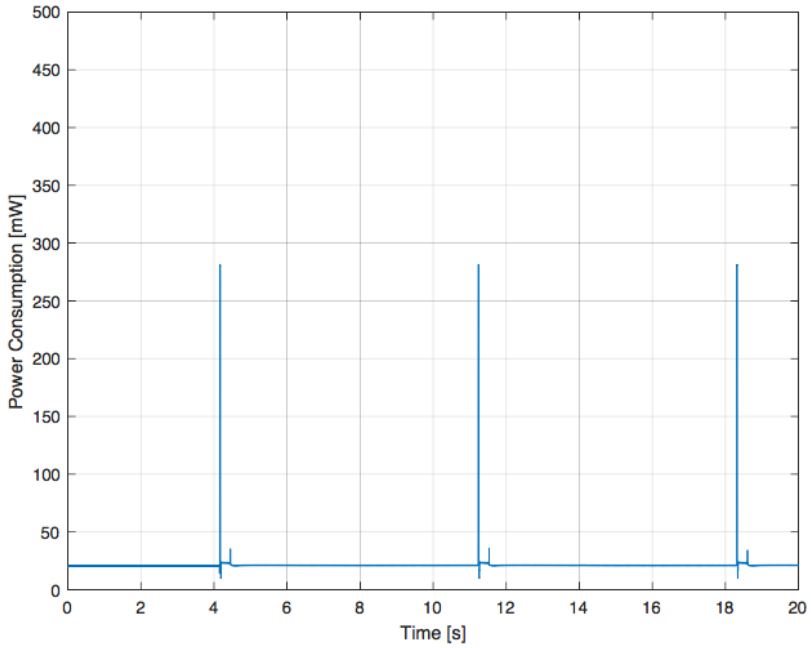

Figure 4.10: Power drain when the radio is on (LoRa mode, $+10dBm$ TX power)

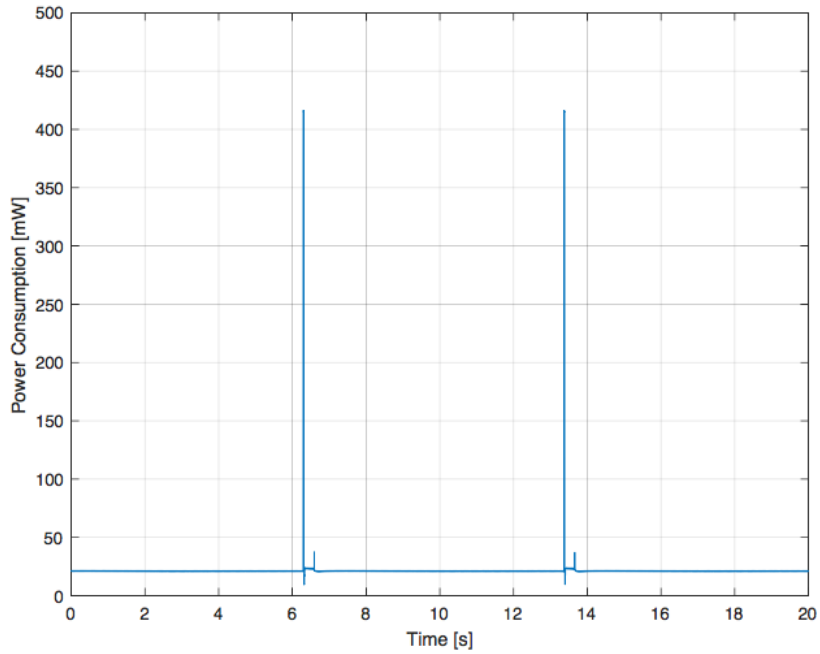

Figure 4.11: Power drain when the radio is on (LoRa mode, $+14dBm$ TX power)

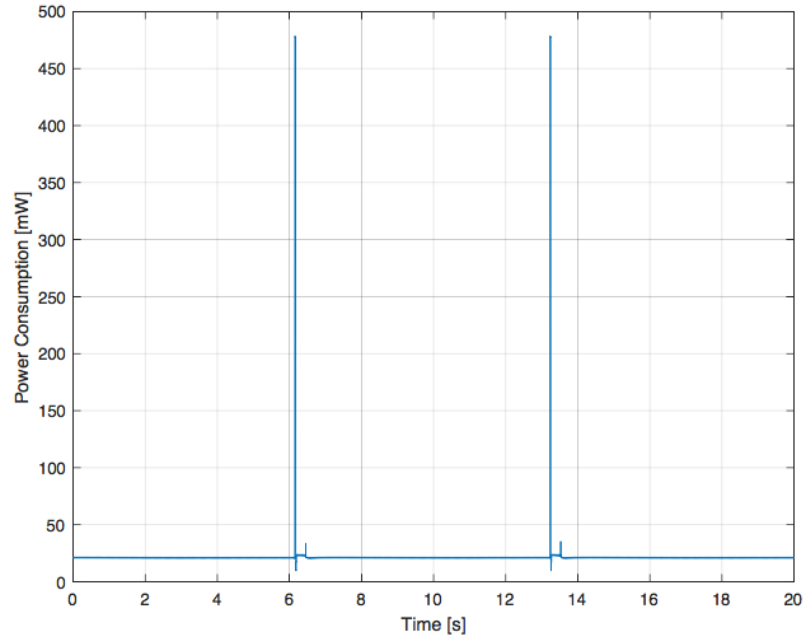

Figure 4.12: Power drain when the radio is on (LoRa mode, $+17dBm$ TX power)

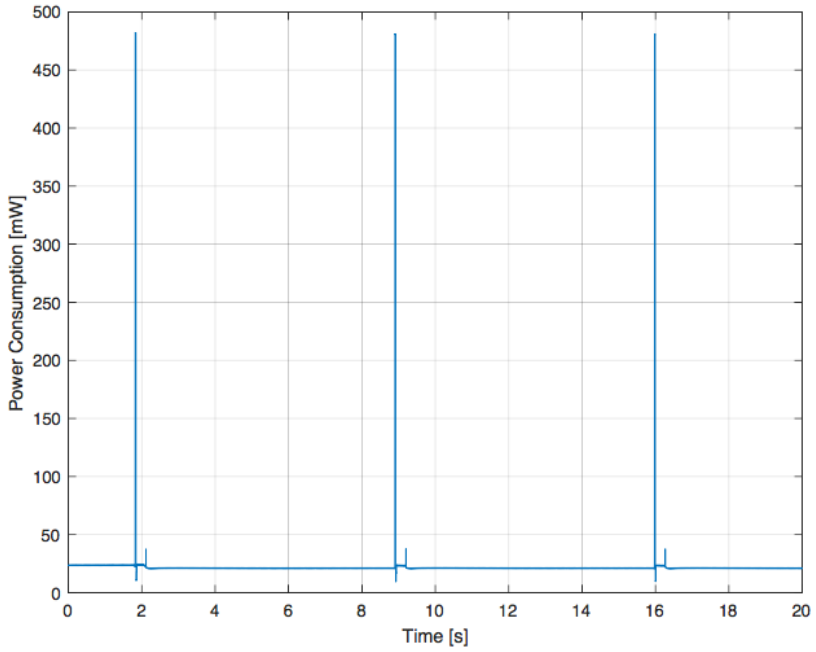

Figure 4.13: Power drain when the radio is on (LoRa mode, $+20dBm$ TX power)

The result of the power analysis in scenario 7 shows that the radio configured in LoRa mode has the same power consumption during listening. The average power drain of the system in receiving mode is approximately $21mW$. The average consumption during transmission is approximately $145mW$ with $0dBm$ transmission power, and the consumption increases as the transmission power is raised. At the maximum, $+20dBm$ transmitting power the system drains $482mW$ of power

4.4.5 Results

A realistic operation scheme of a WuLoRa endnode is demonstrated in Figure 4.14. During the first four seconds, the entire system is in sleep mode, except the wake-up circuit which is always switched on. In the 4th second, a valid wake-up beacon arrives and the wake-up circuit issues an interrupt for the PIC microcontroller. The PIC MCU wakes up from sleep and becomes active.

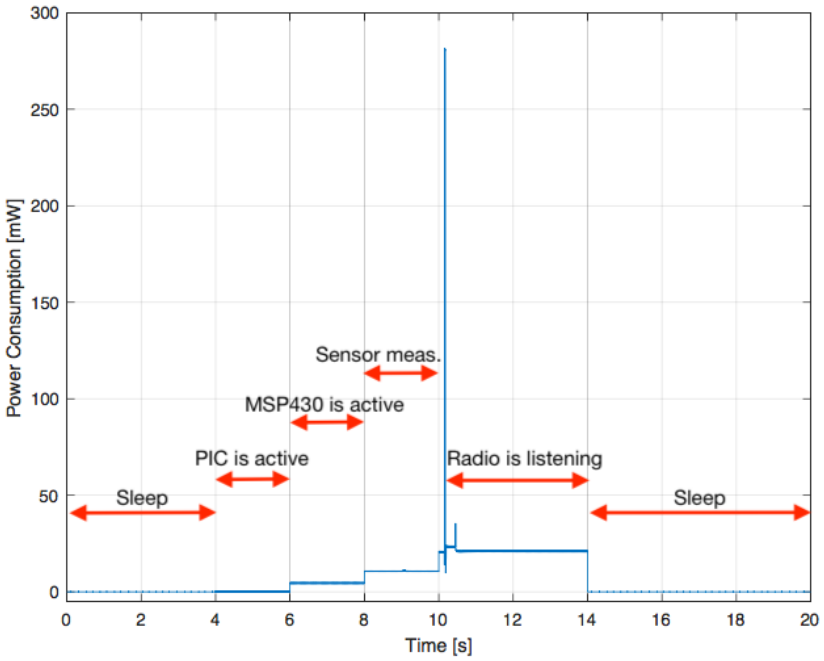

Figure 4.14: Power consumption of system during operation

For demonstration purposes, the PIC waits two seconds in active mode and then wakes up the main power system, including the MSP430 microcontroller.

This event occurs in the 6th second. Again, solely for illustration purposes, the MSP430 microcontroller stays in active mode and waits two seconds. Then it powers up the sensors and polls the sensors via the I^2C interface for measurement data between the 8th and 10th seconds. After polling the sensors, the MSP430 wakes up the main radio and configures it in LoRa mode, with $+10dBm$ transmission power; and performs the transmission of a data packet. After sending out the packet, the radio is switched to listening mode for four seconds, then the entire system goes back to sleep.

Table 4.1 summarizes the power consumption in each scenario of the demonstrated operation scheme.

Time	**Event**	**Power Dissipation**
$0s - 4s$	System sleep	$2.091\mu W$
$4s - 6s$	PIC is active, rest of the system is in sleep	$93.830\mu W$
$6s - 8s$	MSP430 and main power subsystem is active	$4.534mW$
$8s - 10s$	Sensor measurement	$10.671mW$
$10s$	Radio is switched on (LoRa with $+10dBm$ TX power) and sends packet	$282mW$
$10s - 14s$	Radio is listening	$21.011mW$
$14s - 20s$	System sleep	$2.091\mu W$

Table 4.1: Results of power analysis

4.5 Battery Life Estimation

Based on the results of the power analysis presented in Section 4.4.5, one can calculate the battery life of a WuLoRa end-node. The following list summarizes the parameters of such a node:

- The WuLoRa node is equipped with a $800mAh$ Li-Ion battery, which is not charged during operation.
- System is in full sleep in *idle* mode. The always-on subsystem is constantly switched on, however the PIC stays in sleep mode.

- Once every hour, a wake-up beacon is received, and the system wakes up only when a beacon is received.
- After wake-up, the MSP430 is switched on and it performs sensor measurements.
- After performing measurements, the main radio is switched on and the measured data is transmitted to the LoRaWAN network with $+10dBm$ transmission power.
- The radio stays in listening mode for one second after transmission, then the entire system goes back to sleep.

Table 4.2 summarizes the data required to calculate the estimated battery life. The system voltage is $3.0V$.

Event	**Duration**	**Current Drain**	**Consumption**
PIC is active	$0.5s$	$31.28\mu A$	$15.64\mu As$
MCU is active and performs measurements	$1s$	$3.557mA$	$3.557mAs$
LoRa transmission	$0.5s$	$94.0mA$	$47mAs$
LoRa listening	$1s$	$7.0mA$	$7mAs$
System sleep	$3597s$	$0.697\mu A$	$2.507mAs$

Table 4.2: Energy consumption in one hour

Based on the calculated data in Table 4.2, the overall energy consumption is $60.079mAs$ per hour, which adds up to $1441.896mAs$ – or $0.4005mAh$ – per day. Considering a $800mAh$ battery, the entire system would run for 1997 days without interruption, which means roughly 5 and a half years of continuous operation. It is worth mentioning here that the above performed calculation is performed without taking into account the effect of the harvester circuit.

Let's attach a small, $4cm^2$, $500mW$ solar panel to the harvester circuit. If the sun shines for only two hours per day, the harvested energy is not only enough to operate the entire node, but also sufficient to charge the battery.

Chapter 5

Conclusion

The purpose of the project is to describe and develop a state-of-the-art IoT end-node, focusing on ultra-low power consumption alongside with ultra-low latency. The developed WuLoRa node features a solar energy harvester subsystem, various sensors, ultra-low power microcontrollers, nanowatt wake-up circuit and a LoRa-capable radio transceiver.

The preliminary prototype is extensively evaluated, step-by-step. The hardware issues are described and corrected. The sensors are revived, initialized, and configured to obtain correct environmental measurements. The power subsystem is debugged and different power scenarios are set up to test the subsystem. The wake-up circuit is set up and tested. The main radio transceiver is tested in different communication protocols and with different transmission power values.

An extensive power analysis is performed to measure system performance and power consumption in different scenarios. The results of the analysis confirms the effectiveness of the WuLoRa system, and clearly shows that combining a LoRa-enabled IoT end-node with nanowatt wake-up circuit can circumvent the high latency of a Class A LoRa node. Equipping a wake-up circuit negligibly increases the power consumption of the system, and it significantly reduces communication latency while preserving ultra-low power consumption.

Based on the discovered issues of the preliminary prototype, an improved, new WuLoRa prototype is designed and a small batch is manufactured.

5.1 Future Work

Although the outcome of this project is proven to be successful, the WuLoRa IoT end-node can be improved even further. A straightforward way to achieve improvements is to further improve each subsystem, optimize each component

alongside with the printed circuit board to further reduce power consumption, network latency and node size.

However, a less obvious but greatly promising idea would be to try out and experiment with brand-new, state-of-the-art System-on-Chip (SoC) solutions. ST Microelectronics, a leading microcontroller manufacturer company teamed up with Semtech to develop a new SoC component featuring a LoRa-enabled radio module from Semtech together with the state-of-the-art, Cortex M-core ultra-low power microcontroller from ST. The outcome of this collaboration is the new CMWX1ZZABZ[1] chip manufactured by Murata Manufacturing Co. It encapsulates an SX1276 LoRa-enabled transceiver together with a STM32L072 ultra-low power Cortex-M0+ core microcontroller on a single SoC. The STM32L0 series microcontrollers are specifically developed for ultra-low power applications and they feature numerous low-power modes, furthermore the L-series microcontrollers from ST are constantly leading in the ULPBENCH[2] benchmarks with their exceptionally high ULPMark scores[3].

Experimenting with new System-on-Chips specifically targeted for ultra-low power IoT applications would not only reduce the required space on the printed circuit board, but would also provide a simplified system design, moreover they would even question the need of a secondary microcontroller for the wake-up circuit.

[1] Murata CMWX1ZZABZ - http://wireless.murata.com/eng/products/rf-modules-1/lpwa/type-abz.html
[2] ULPBENCH - http://www.eembc.org/ulpbench/about.php
[3] ULPMark-CP scores - http://www.eembc.org/ulpbench/index.php

Bibliography

[1] IHS, "IoT Platforms - Enabling the Internet of Things," Whitepaper, IHS Markit, 2016.

[2] "Moore's law." https://en.wikipedia.org/wiki/Moore%27s_law.

[3] "LoRa Alliance." https://www.lora-alliance.org.

[4] "SX1276 - LoRa-enabled radio transceiver by Semtech." http://www.semtech.com/wireless-rf/rf-transceivers/sx1276/.

[5] "Semtech SX1276 Datasheet." http://www.semtech.com/images/datasheet/sx1276.pdf.

[6] "HopeRF - RFM95W Transceiver Module." http://www.hoperf.com/rf_transceiver/lora/RFM95W.html.

[7] F. A. Aoudia, M. Magno, M. Gautier, O. Berder, and L. Benini, "A low latency and energy efficient communication architecture for heterogeneous long-short range communication," in *2016 Euromicro Conference on Digital System Design (DSD)*, pp. 200–206, Aug 2016.

[8] M. Magno, V. Jelicic, B. Srbinovski, V. Bilas, E. Popovici, and L. Benini, "Design, implementation, and performance evaluation of a flexible low-latency nanowatt wake-up radio receiver," *IEEE Transactions on Industrial Informatics*, vol. 12, pp. 633–644, April 2016.

[9] "Microchip PIC12LF1552 Datasheet." http://ww1.microchip.com/downloads/en/DeviceDoc/40001674F.pdf.

[10] "Wikipedia - Ferroelectric RAM." https://en.wikipedia.org/wiki/Ferroelectric_RAM.

[11] "Texas Instruments - MSP430FR5969 Datasheet." http://www.ti.com/lit/ds/symlink/msp430fr5969.pdf.

[12] L. Sigrist, A. Gomez, R. Lim, S. Lippuner, M. Leubin, and L. Thiele, "Measurement and validation of energy harvesting iot devices," in *Design, Automation Test in Europe Conference Exhibition (DATE), 2017*, pp. 1159–1164, March 2017.

[13] M. Magno, F. A. Aoudia, M. Gautier, O. Berder, and L. Benini, "Wulora: An energy efficient iot end-node for energy harvesting and heterogeneous communication," in *Design, Automation Test in Europe Conference Exhibition (DATE), 2017*, pp. 1528–1533, March 2017.

[14] "Texas Instruments - BQ22570 Energy Harvester Datasheet." `http://www.ti.com/lit/ds/symlink/bq25570.pdf`.

[15] "ST Microelectronics - STC3115 Gas Gauge IC Datasheet." `www.st.com/resource/en/datasheet/stc3115.pdf`.

[16] "Texas Instruments - TPS62733 Datasheet." `http://www.ti.com/lit/ds/symlink/tps62733.pdf`.

[17] "InvenSense - MPU-9250 Datasheet." `https://www.invensense.com/wp-content/uploads/2015/02/PS-MPU-9250A-01-v1.1.pdf`.

[18] Dennis Hudgins, "Precision, Low-Side Current Measurement," TI Tech-Notes, Texas Instruments, December 2016.

Appendix A

Repository Organization

The project root folder contains five folders. The `code` directory contains the source code for the microcontrollers. The `literature` folder contains research documents and papers. The raw files of the power analysis alongside with the RocketLogger script files are located in the `matlab` folder. The `pcb` directory contains the hardware design files of the preliminary prototype and the newly designed prototype. The report folder contains the project report, presentation and related images, figures.

```
LoRa/
  |── code/
  |── literature/
  |── matlab/
  |── pcb/
  `── report/
```

Figure A.1: Repository organization

Appendix B

Schematics of Prototype Redesign

The schematic document of the redesigned prototype is included in the following pages.

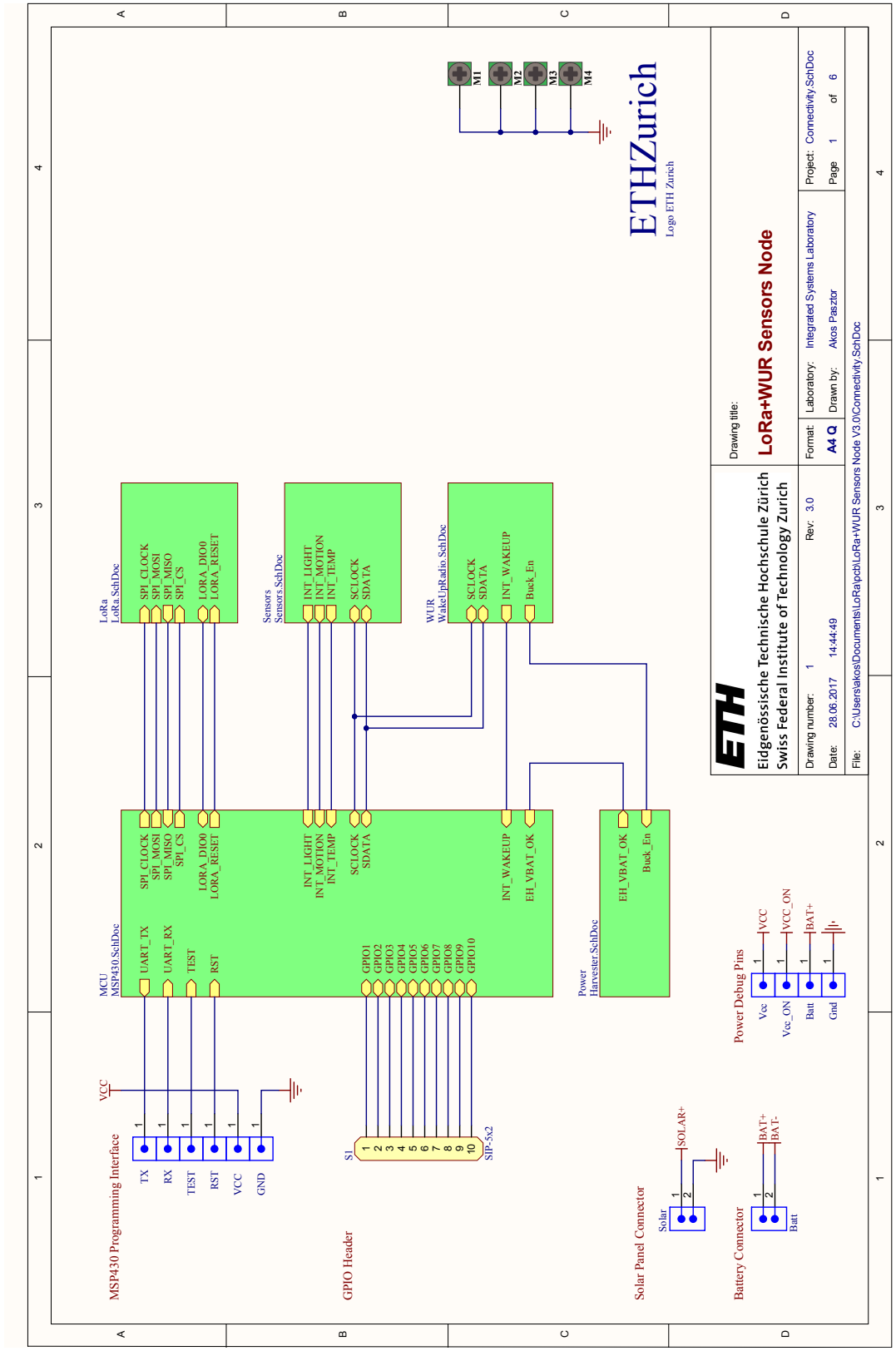
ETHZurich
Logo ETH Zurich
M1
M2
M3
M4
LoRa
LoRa.SchDoc
SPI_CLOCK
SPI_MOSI
SPI_MISO
SPI_CS
LORA_DIO0
LORA_RESET
Sensors
Sensors.SchDoc
INT_LIGHT
INT_MOTION
INT_TEMP
SCLOCK
SDATA
WUR
WakeUpRadio.SchDoc
INT_WAKEUP
Buck_En
MCU
MSP430.SchDoc
UART_TX
UART_RX
TEST
RST
GPIO1
GPIO2
GPIO3
GPIO4
GPIO5
GPIO6
GPIO7
GPIO8
GPIO9
GPIO10
EH_VBAT_OK
Power
Harvester.SchDoc
MSP430 Programming Interface
TX
RX
TEST
RST
VCC
GND
VCC
GPIO Header
S1
SIP-5x2
Solar Panel Connector
Solar
SOLAR+
Battery Connector
Batt
BAT+
BAT-
Power Debug Pins
Vcc
Vcc_ON
Batt
Gnd
VCC
VCC_ON
BAT+
Eidgenössische Technische Hochschule Zürich
Swiss Federal Institute of Technology Zurich
Drawing title:
LoRa+WUR Sensors Node
Drawing number: 1
Rev: 3.0
Format: A4 Q
Laboratory: Integrated Systems Laboratory
Drawn by: Akos Pasztor
Project: Connectivity.SchDoc
Page 1 of 6
Date: 28.06.2017 14:44:49
File: C:\Users\akos\Documents\LoRa\pcb\LoRa+WUR Sensors Node V3.0\Connectivity.SchDoc

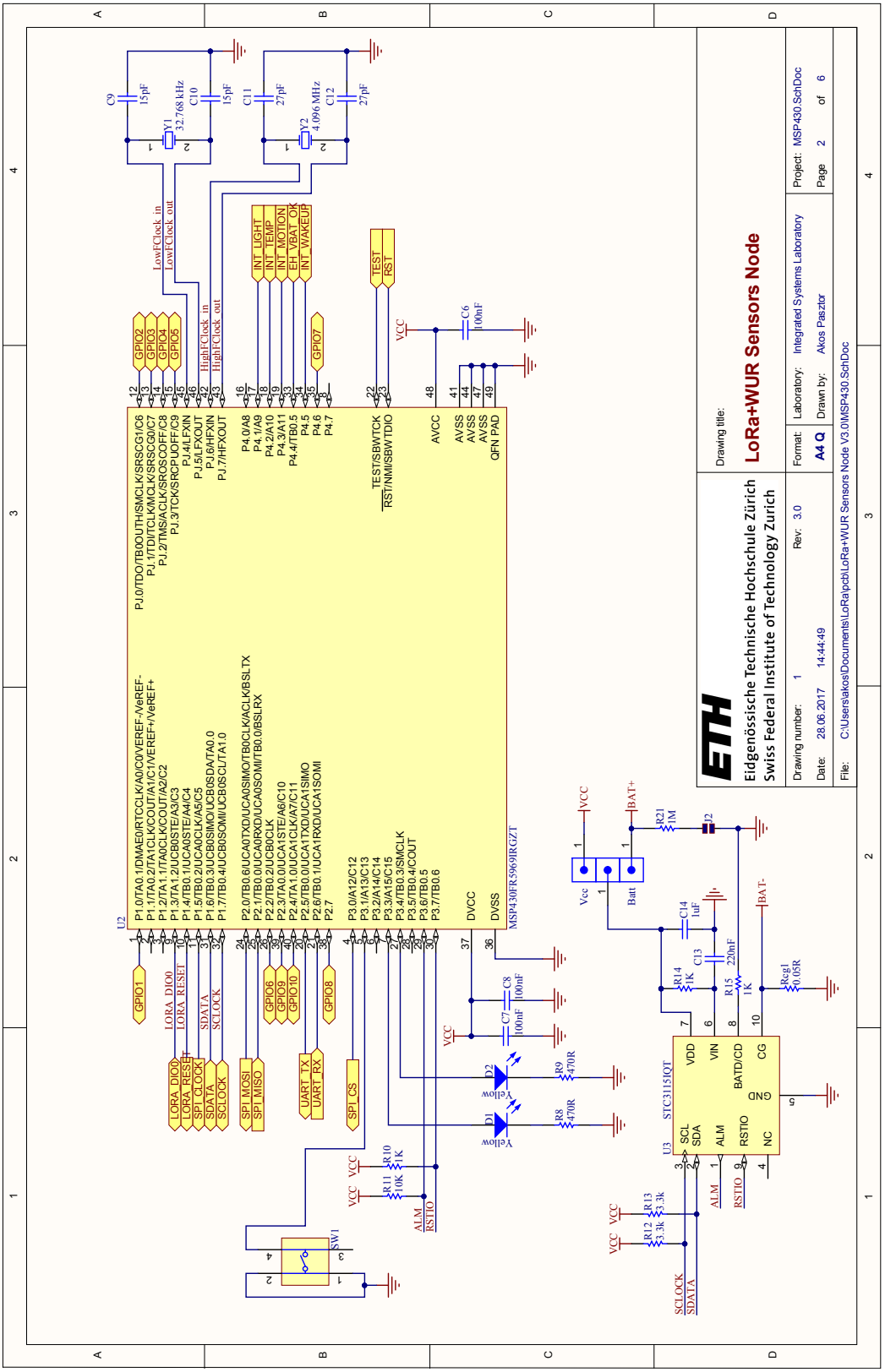
ETH
Eidgenössische Technische Hochschule Zürich
Swiss Federal Institute of Technology Zurich
Drawing title:
LoRa+WUR Sensors Node
Drawing number: 1
Rev: 3.0
Format: A4 Q
Laboratory: Integrated Systems Laboratory
Drawn by: Akos Pasztor
Project: MSP430.SchDoc
Page 2 of 6
Date: 28.06.2017 14:44:49
File: C:\Users\akos\Documents\LoRa\pcb\LoRa+WUR Sensors Node V3.0\MSP430.SchDoc
U2
MSP430FR5969IRGZT
U3
STC3115IQT
Y1 32.768 kHz
Y2 4.096 MHz
C9 15pF
C10 15pF
C11 27pF
C12 27pF
C6 100nF
C7 100nF
C8 100nF
C13 220nF
C14 1uF
R21 1M
R14 1K
R15 1K
R10 1K
R11 10K
R12 3.3k
R13 3.3k
R9 470R
R8 470R
Reg1 0.05R
SW1
J2
D1 Yellow
D2 Yellow
LowFClock_in
LowFClock_out
HighFClock_in
HighFClock_out
INT_LIGHT
INT_TEMP
INT_MOTION
EH_VBAT_OK
INT_WAKEUP
TEST
RST
LORA_DIO0
LORA_RESET
SPI_CLOCK
SDATA
SCLOCK
SPI_MOSI
SPI_MISO
UART_TX
UART_RX
SPI_CS
ALM
RSTIO
VCC
BAT+
BAT-
Vcc
Batt
SCL
SDA
VDD
VIN
BATD/CD
CG
GND
NC

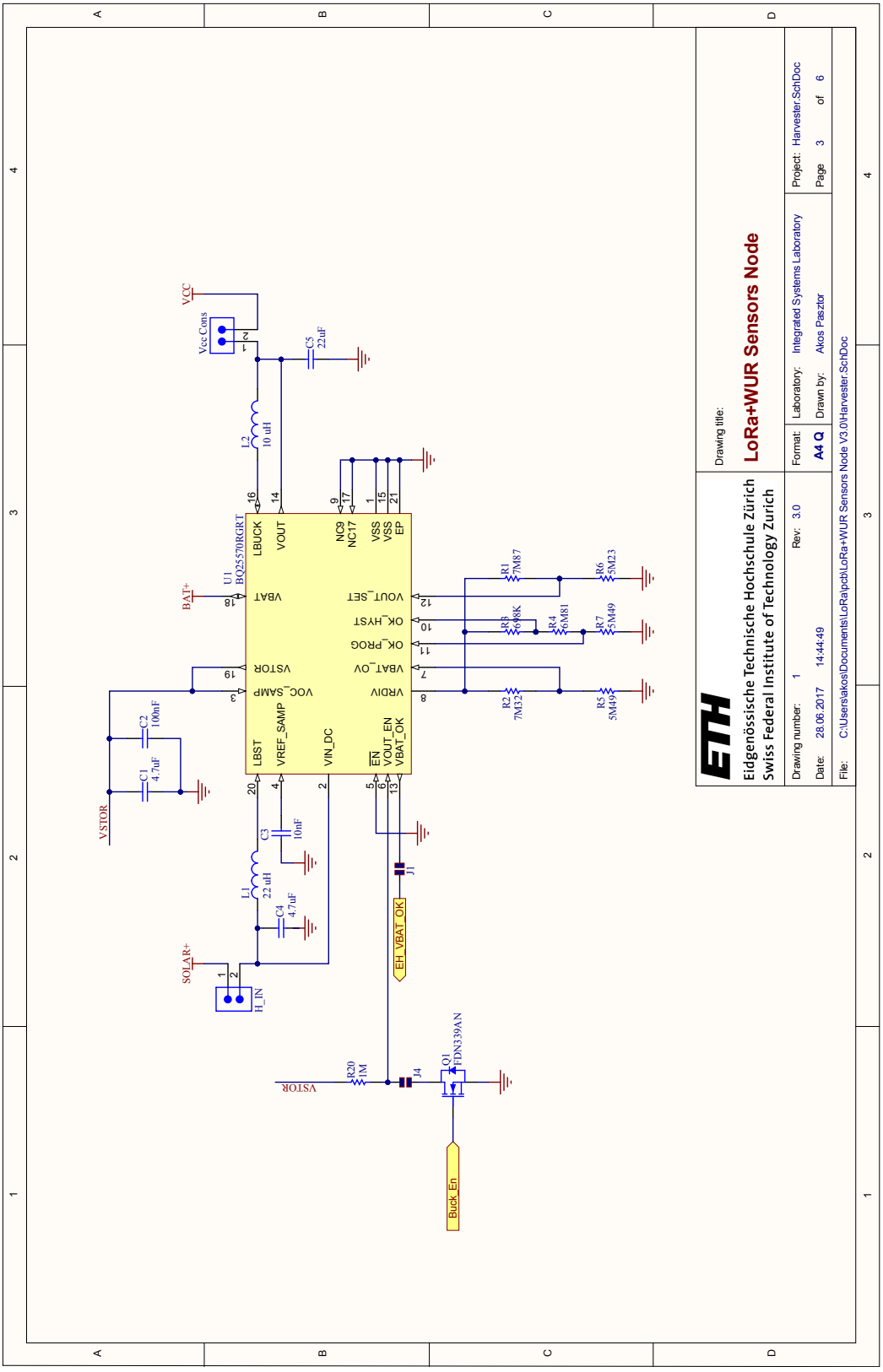
Eidgenössische Technische Hochschule Zürich
Swiss Federal Institute of Technology Zurich
Drawing title:
LoRa+WUR Sensors Node
Format: A4 Q
Laboratory: Integrated Systems Laboratory
Drawn by: Akos Pasztor
Project: Harvester.SchDoc
Page 3 of 6
Drawing number: 1
Rev: 3.0
Date: 28.06.2017 14:44:49
File: C:\Users\akos\Documents\LoRa\pcb\LoRa+WUR Sensors Node V3.0\Harvester.SchDoc
U1 BQ25570RGRT
LBUCK
VOUT
VBAT
VOUT_SET
OK_HYST
OK_PROG
VBAT_OV
VRDIV
VSTOR
VOC_SAMP
LBST
VREF_SAMP
VIN_DC
EN
VOUT_EN
VBAT_OK
NC9
NC17
VSS
VSS
EP
VCC
Vcc Conn
BAT+
SOLAR+
H_IN
VSTOR
L1 22 uH
L2 10 uH
C1 4.7uF
C2 100nF
C3 10nF
C4 4.7uF
C5 22uF
R1 7M87
R2 7M32
R3 698K
R4 6M81
R5 5M49
R6 5M23
R7 5M49
R20 1M
J1
J4
Q1 FDN339AN
EH_VBAT_OK
Buck_En

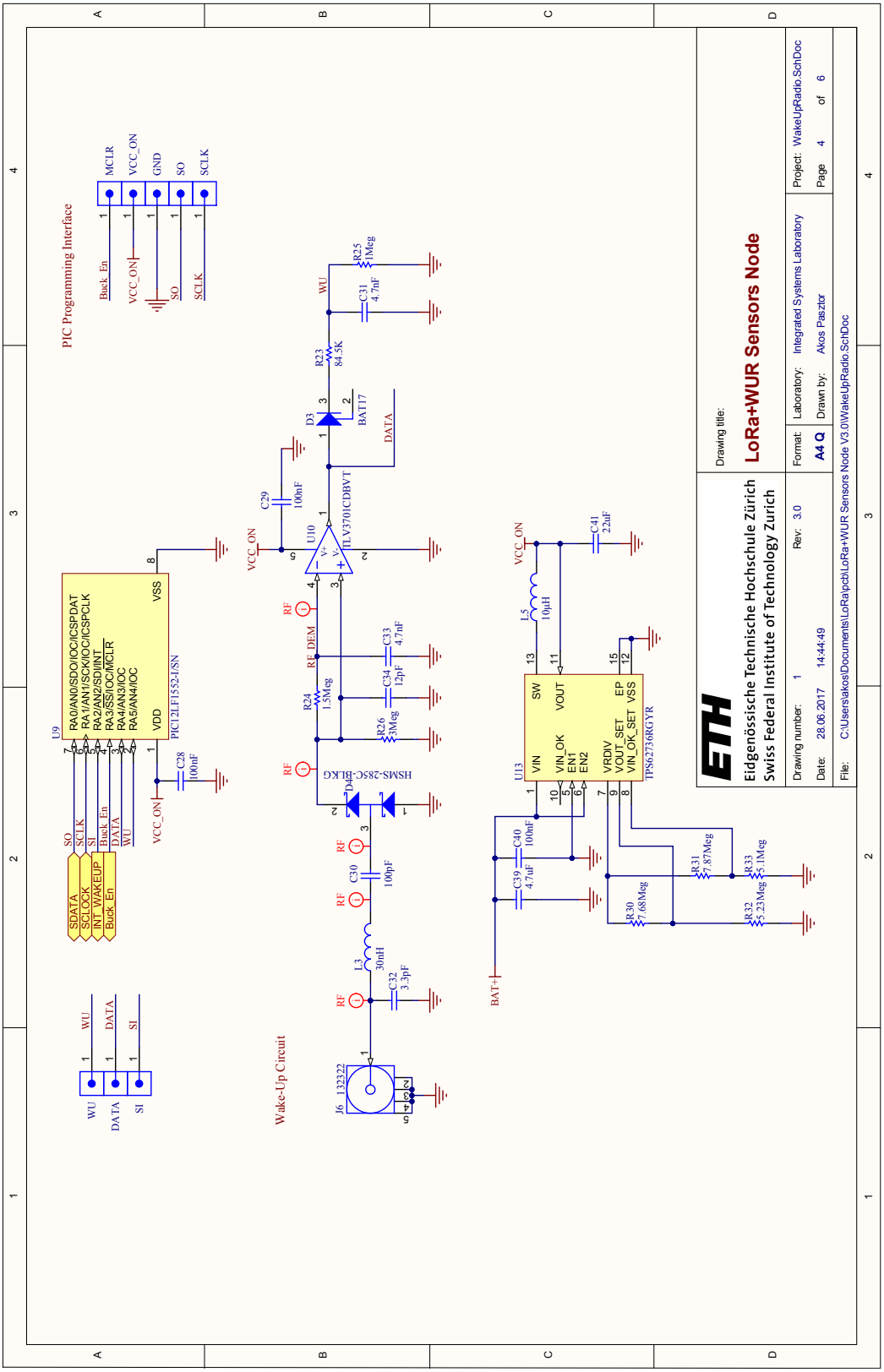
PIC Programming Interface
MCLR
VCC_ON
GND
SO
SCLK
Buck_En
U9
PIC12LF1552-I/SN
RA0/AN0/SDO/ICC/ICSPDAT
RA1/AN1/SCK/IOC/ICSPCLK
RA2/AN2/SDI/INT
RA3/SS/IOC/MCLR
RA4/AN3/IOC
RA5/AN4/IOC
VDD
VSS
C28
100nF
SDATA
SCLOCK
INT_WAKEUP
Buck_En
DATA
WU
SI
Wake-Up Circuit
U10
TLV3701CDBVT
C29
100nF
D3
BAT17
R23
84.5K
R25
1Meg
C31
4.7nF
D4
HSMS-285C-BLKG
R24
1.5Meg
R26
3Meg
C33
4.7nF
C34
12pF
C30
100pF
L3
30nH
C32
3.3pF
J6 132322
U13
TPS62736RGYR
L5
10µH
C41
22uF
C40
100nF
C39
4.7uF
R31
7.87Meg
R32
5.23Meg
R33
5.1Meg
R30
7.68Meg
BAT+
Eidgenössische Technische Hochschule Zürich
Swiss Federal Institute of Technology Zurich
Drawing title:
LoRa+WUR Sensors Node
Drawing number: 1
Rev: 3.0
Format: A4 Q
Laboratory: Integrated Systems Laboratory
Drawn by: Akos Pasztor
Project: WakeUpRadio.SchDoc
Page 4 of 6
Date: 28.06.2017 14:44:49
File: C:\Users\akos\Documents\LoRa\pcb\LoRa+WUR Sensors Node V3.0\WakeUpRadio.SchDoc

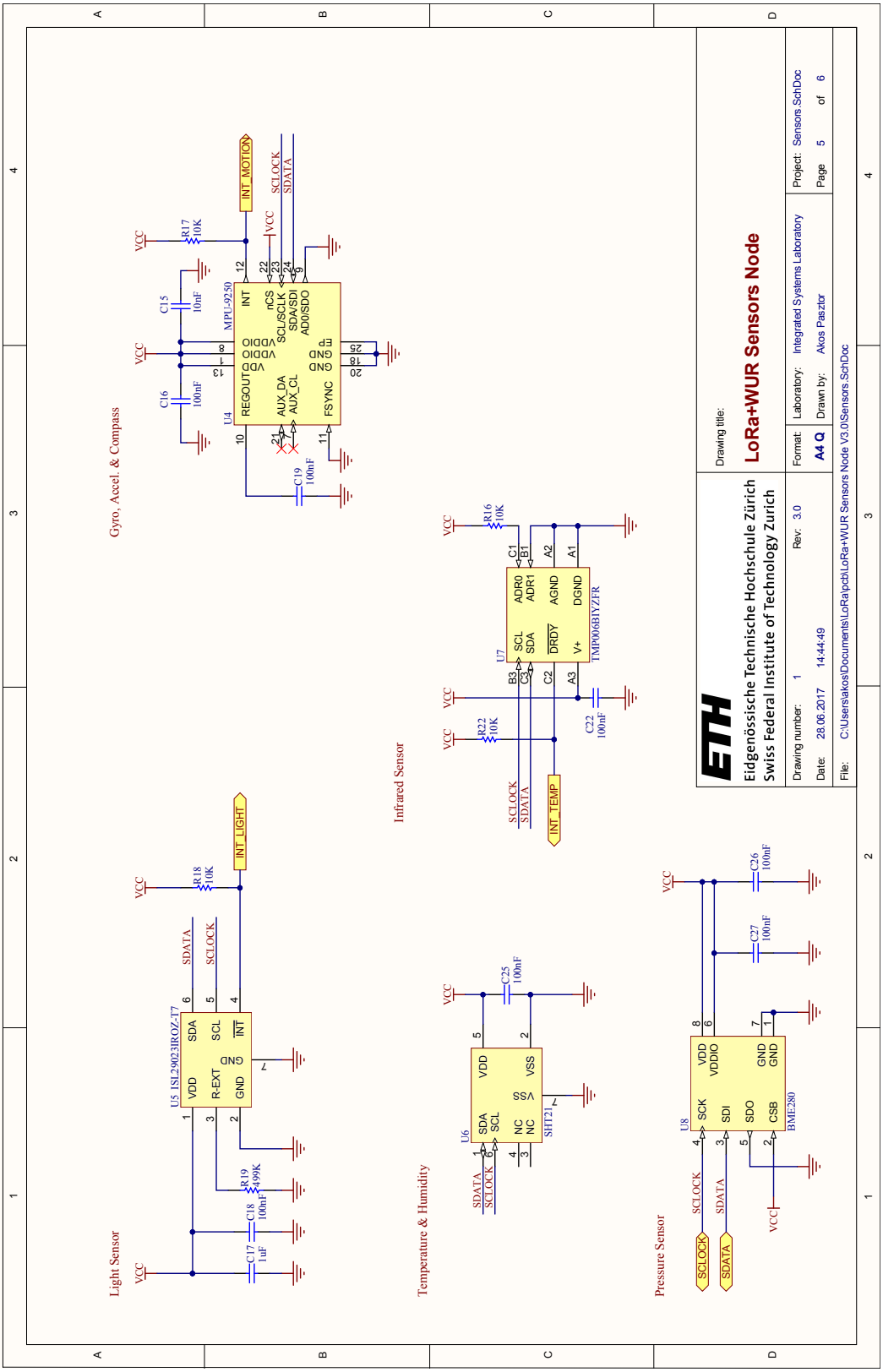
Gyro, Accel. & Compass
Light Sensor
Infrared Sensor
Temperature & Humidity
Pressure Sensor
MPU-9250
U5 ISL29023IROZ-T7
U6 SHT21
U7 TMP006B1YZFR
U8 BME280
INT_MOTION
INT_LIGHT
INT_TEMP
SCLOCK
SDATA
VCC
Eidgenössische Technische Hochschule Zürich
Swiss Federal Institute of Technology Zurich
Drawing title:
LoRa+WUR Sensors Node
Drawing number: 1
Rev: 3.0
Date: 28.06.2017 14:44:49
Format: A4 Q
Laboratory: Integrated Systems Laboratory
Drawn by: Akos Pasztor
Project: Sensors.SchDoc
Page 5 of 6
File: C:\Users\akos\Documents\LoRa\pcb\LoRa+WUR Sensors Node V3.0\Sensors.SchDoc

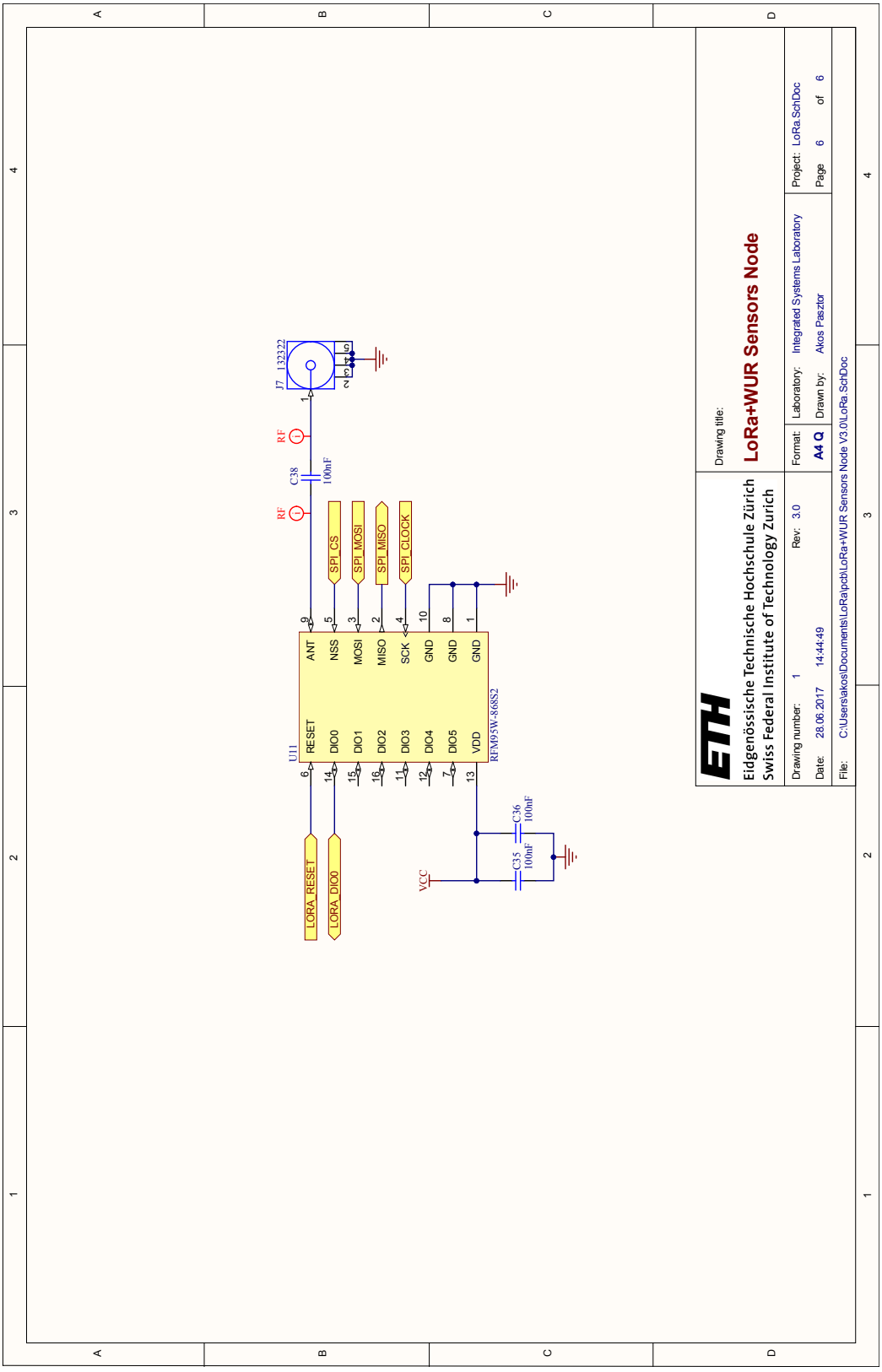
A
B
C
D
1
2
3
4
J7 132322
RF
C38
100nF
RF
U11
RESET
DIO0
DIO1
DIO2
DIO3
DIO4
DIO5
VDD
ANT
NSS
MOSI
MISO
SCK
GND
GND
GND
RFM95W-868S2
SPI_CS
SPI_MOSI
SPI_MISO
SPI_CLOCK
LORA_RESET
LORA_DIO0
VCC
C36
100nF
C35
100nF
ETH
Eidgenössische Technische Hochschule Zürich
Swiss Federal Institute of Technology Zurich
Drawing title:
LoRa+WUR Sensors Node
Drawing number: 1
Rev: 3.0
Date: 28.06.2017 14:44:49
Format: A4 Q
Laboratory: Integrated Systems Laboratory
Drawn by: Akos Pasztor
Project: LoRa.SchDoc
Page 6 of 6
File: C:\Users\akos\Documents\LoRa\pcb\LoRa+WUR Sensors Node V3.0\LoRa.SchDoc

Appendix C

PCB Layout of Prototype Redesign

The printed circuit board layout of the redesigned prototype is included in the following pages.

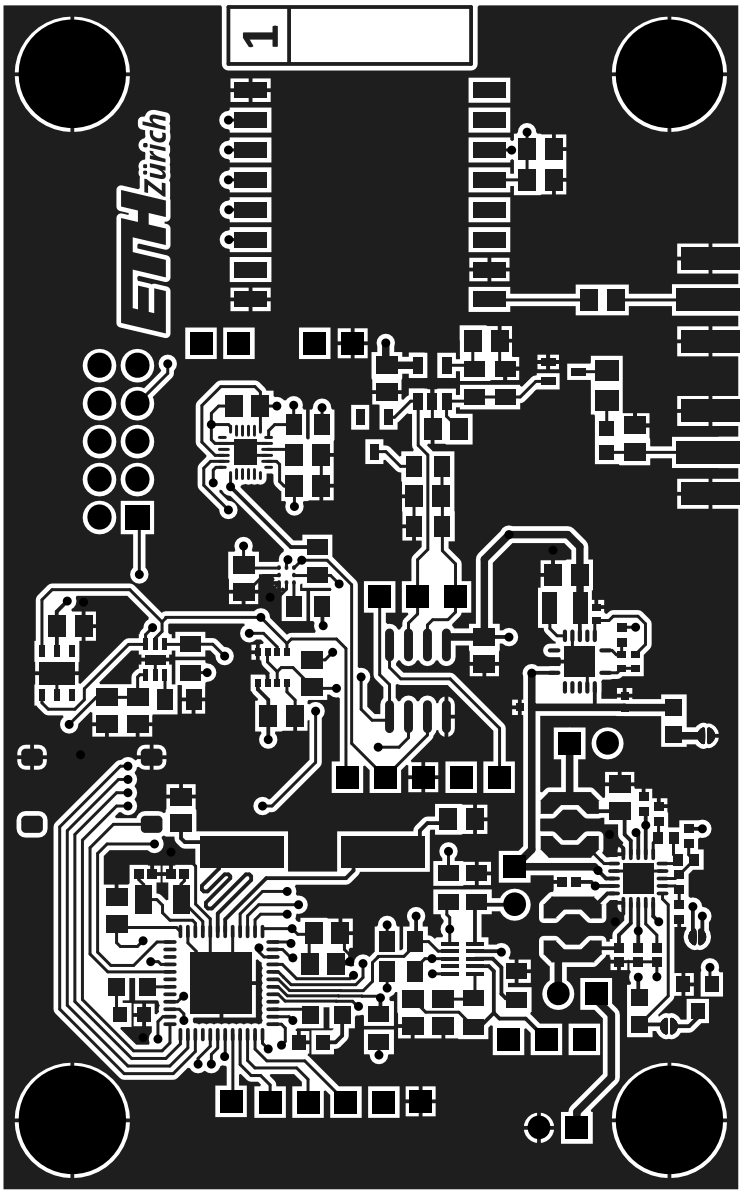
1
ETH Zürich

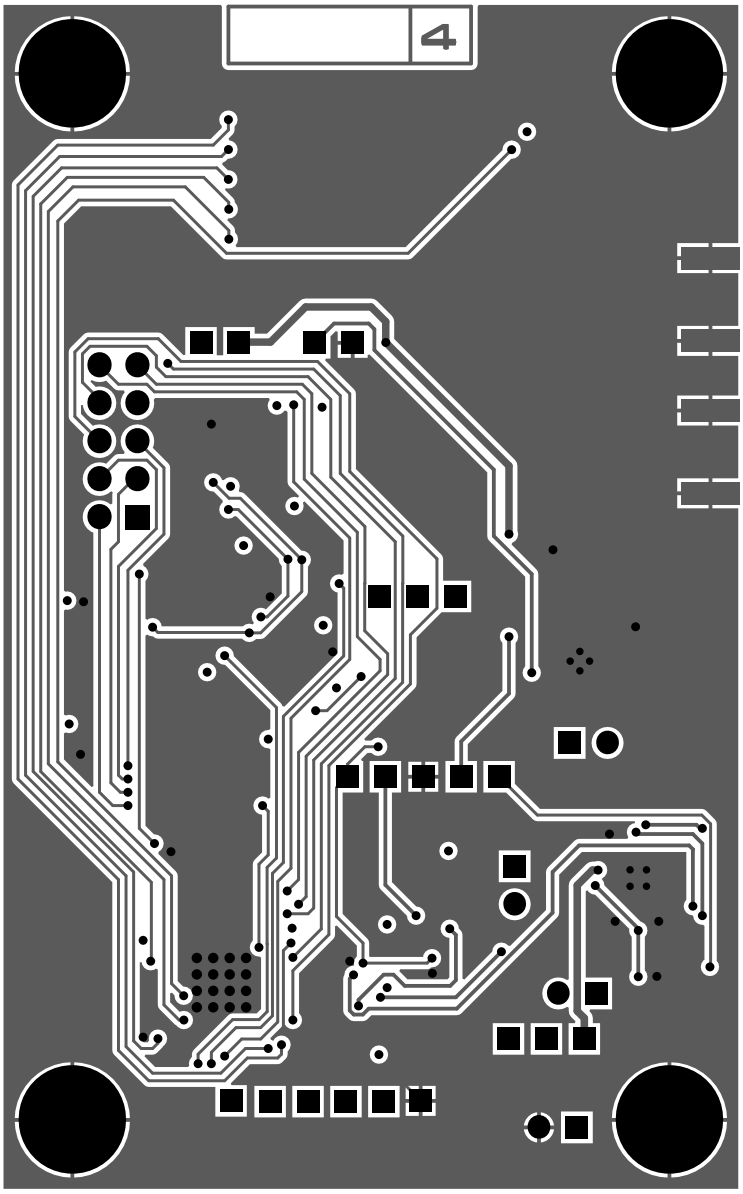
4

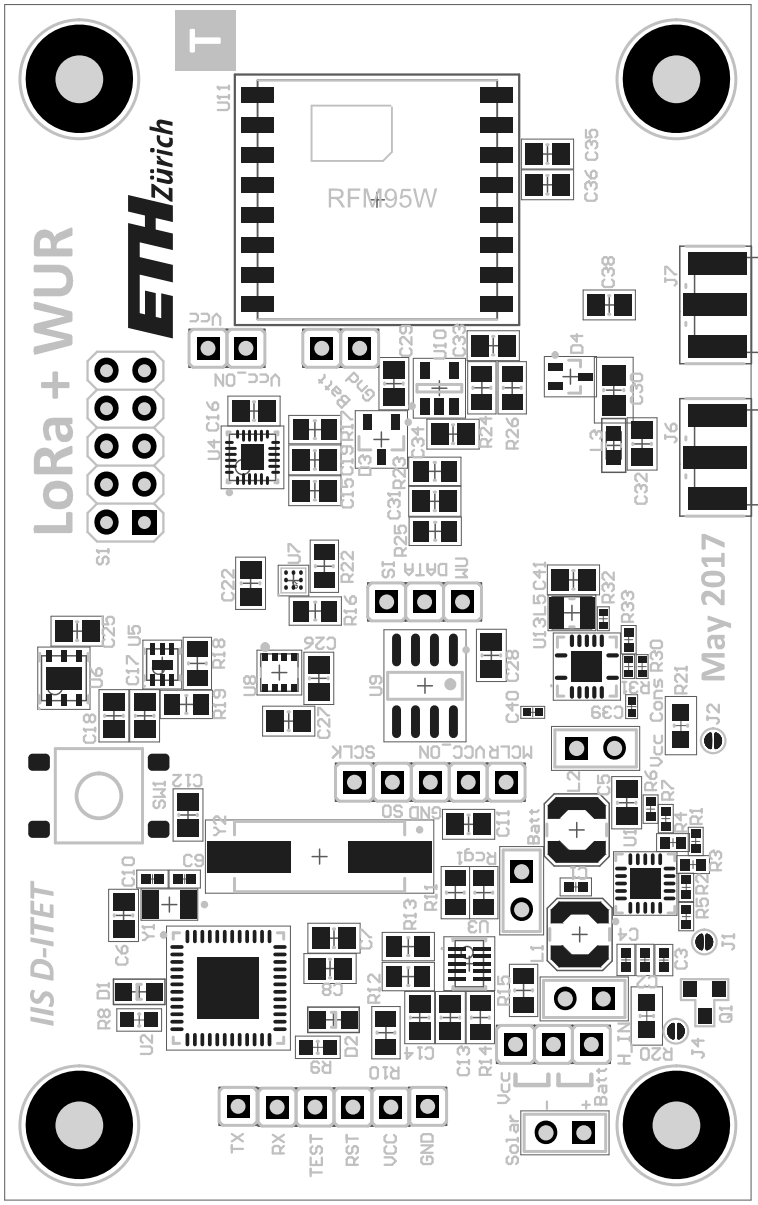
LoRa + WUR
ETH Zürich
IIS D-ITET
May 2017
RFM95W
TX
RX
TEST
RST
VCC
GND
Solar
Batt

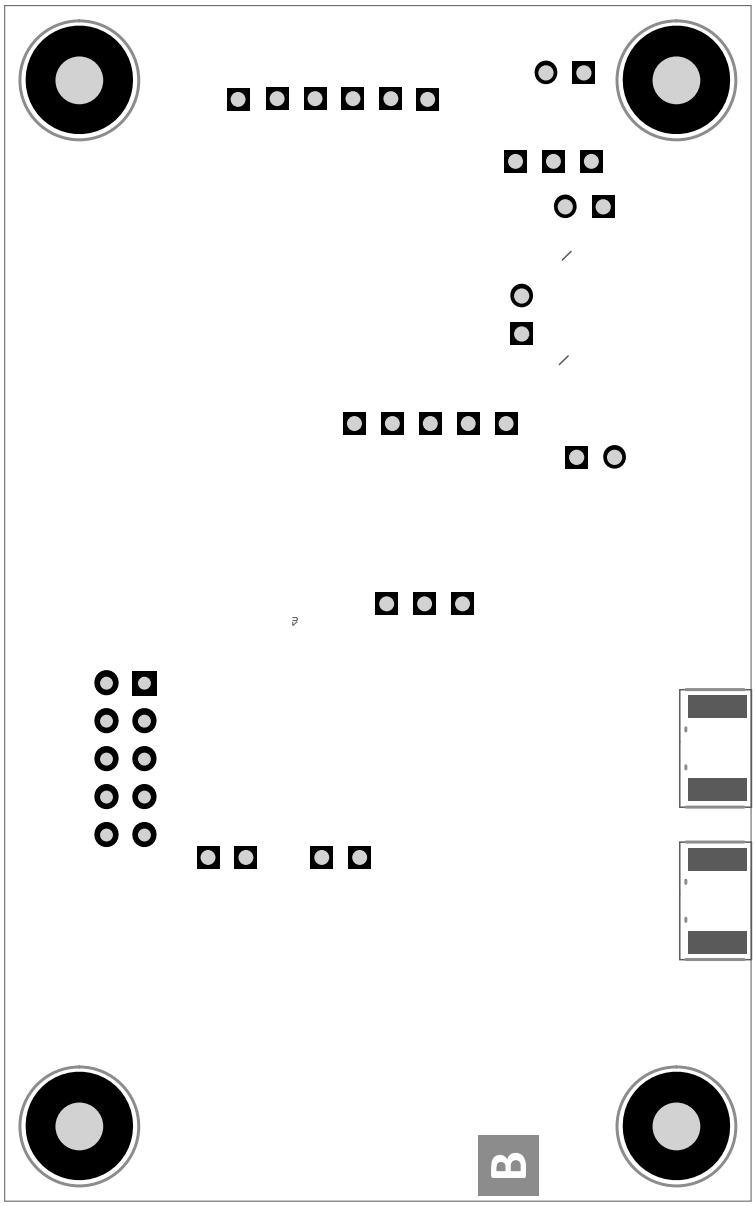
B

Appendix D

Bill of Materials

The exported bill of materials document is included in the following pages.

Appendix D. Bill of Materials

Designator	Comment	Footprint	LibRef	Manufacturer Part Number 1	Quantity
C1, C4, C39	CAP 4.7uF 6.3V 0402(1005)	CAPC0402(1005)60_N, CAPC0402(1005)60_N, CAPC0402(1005)60_L	CMP-1034-02136-1		3
C2, C40	CAP 100nF 25V 0402(1005)	CAPC0402(1005)60_N, CAPC0402(1005)60_L	CMP-1034-02072-1	04023C104KAT2A	2
C3	CAP 10nF 25V 0402(1005)	CAPC0402(1005)60_N	CMP-1034-01880-1	04023C103KAT2A	1
C5, C41	CAP 22uF 6.3V 0805(2012)	CAPC0805(2012)145_N	CMP-1036-04939-1	08056D226MAT2A	2
C6, C7, C8, C16, C18, C19, C22, C25, C26, C27, C28, C29, C35, C36, C38	CAP 100nF 16V 0805(2012)	CAPC0805(2012)145_N	CMP-1036-04401-1	C0805C104K4RACTU	15
C9, C10	CAP 15pF 25V 0402(1005)	CAPC0402(1005)60_N	CMP-1034-00808-1	04023A150JAT2A	2
C11, C12	CAP 27pF 10V 0805(2012)	CAPC0805(2012)100_N	CMP-1036-01312-1	VJ0805A270KXQCW1BC	2
C13	CAP 220nF 16V 0805(2012)	CAPC0805(2012)145_N	CMP-1036-04536-1	0805YC224MAT2A	1
C14, C17	CAP 1uF 16V 0805(2012)	CAPC0805(2012)145_N	CMP-1036-04748-1	0805YC105MAT2A	2
C15	CAP 10nF 16V 0805(2012)	CAPC0805(2012)100_N	CMP-1036-03818-1	0805YC103JAT2A	1
C30	CAP 100pF 16V 0805(2012)	CAPC0805(2012)100_M	CMP-1036-01943-1	C0805C101K4GACTU	1
C31, C33	CAP 4.7nF 16V 0805(2012)	CAPC0805(2012)145_N	CMP-1036-03565-1	0805YA472KAT2A	2
C32	CAP 3.3pF 10V 0805(2012)	CAPC0805(2012)75_N	CMP-1036-00386-1	VJ0805A3R3BXQCW1BC	1
C34	CAP 12pF 25V 0805(2012)	CAPC0805(2012)100_N	CMP-1036-00938-1	08053A120JAT2A	1
D1, D2	150080YS75000	0805_A	CMP-1426-00012-1	150080YS75000	2
D3	BAT17	INF-SOT23_N	CMP-1154-00014-1		1
D4	HSMS-285C-BLKG	INF-SOT323_N	CMP-00132-1	HSMS-285C-BLKG	1
H_IN, X7, X8, X19	H_IN, Batt, Solar, Vcc Cons	Pin Header, 1x2	CMP-00100-1	68000-102HLF	4
J1, J2, J4	Solder Jumper	Small Solder Jumper	CMP-00005-1		3
J6, J7	132322	132322	CMP-00118-1	132322	2
L1	LPS4018-223MR	COILCRAFT-IND-LPS4018	CMP-00081-1	LPS4018-223MRB	1
L2	LPS4018-103MR	COILCRAFT-IND-LPS4018	CMP-00083-1	LPS4018-103MRB	1
L3	LQW18AN30NJ00D	INDC0603(1608)_N	CMP-00133-1	LQW18AN30NJ00D	1
L5	1239AS-H-100M=P2	INDC2520X10L	CMP-00241-1	1239AS-H-100M=P2	1
Q1	FDN339AN	FDN339AN	FDN339AN		1
R1, R31	7M87, 7M87 1% 0402(1005)	RESC0402(1005)_N, RESC0402(1005)_L	CMP-1011-00950-1	CRCW04027M87FKED	2
R2	7M32	RESC0402(1005)_N	CMP-1011-00947-1	CRCW04027M32FKED	1
R3	698K	RESC0402(1005)_M	CMP-1011-00832-1	CRCW0402698KFKTD	1
R4	6M81	RESC0402(1005)_M	CMP-1011-00944-1	CRCW04026M81FKED	1
R5, R7	5M49	RESC0402(1005)_N	CMP-1011-00933-1	CRCW04025M49FKED	2
R6, R32	5M23, 5M23 1% 0402(1005)	RESC0402(1005)_N, RESC0402(1005)_L	CMP-1011-00931-1	CRCW04025M23FKED	2
R8, R9	470R	RESC0603(1608)_N	CMP-1012-00066-1	CRCW0603470RJNTA	2
R10, R14, R15	1K 1% 0805(2012)	RESC0805(2012)_N	CMP-1013-00510-1	CRCW08051K00FKTA	3
R11, R16, R17, R18, R22	10K 1% 0805(2012)	RESC0805(2012)_N	CMP-1013-00623-1	CR0805-FX-1002ELF	5
R12, R13	3K3 1% 0805(2012)	RESC0805(2012)_N	CMP-1013-00567-1	RC0805FR-073K3L	2
R19	499K 1% 0805(2012)	RESC0805(2012)_N	CMP-1013-00815-1	CRCW0805499KFKTA	1
R20, R21	1M	RESC0603(1608)_M	CMP-1012-00850-1	CRCW06031M02FKTA	2
R23	84K5 1% 0805(2012)	RESC0805(2012)_N	CMP-1013-00728-1	CRCW080584K5FKTA	1
R24	1M5 1% 0805(2012)	RESC0805(2012)_N	CMP-1013-00867-1	CRCW08051M50FKTA	1
R25	1M 1% 0805(2012)	RESC0805(2012)_N	CMP-1013-00849-1	CR0805-FX-1004-ELF	1
R26	3M 1% 0805(2012)	RESC0805(2012)_N	CMP-1013-00901-1	CRCW08053M00FKEA	1
R30	7M68 1% 0402(1005)	RESC0402(1005)_L	CMP-1011-00949-1	CRCW04027M68FKED	1
R33	5M1 1% 0402(1005)	RESC0402(1005)_N	CMP-1011-00929-1	CRCW04025M10FKTD	1
Rcg1	UCR10EVHFSR050	RESC0805(2012)_N	CMP-00129-1	UCR10EVHFSR050	1
S1	SIP-5x2	SIP-5x2	SIP-5x2		1
SW1	ADTSM62RVTR	SW_DTSM-62N	CMP-00033-1	ADTSM62RVTR	1
U1	BQ25570RGRT	QFN50P350X350X100_HS-21L	CMP-00082-2	BQ25570RGRT	1
U2	MSP430FR5969IRGZT	QFN-48-7x7-4.1x4.1_N	CMP-00055-1	MSP430FR5969IRGZT	1
U3	STC3115IQT	SON50P200X60-10N	CMP-00128-1	STC3115IQT	1
U4	MPU-9250	MPU-9250	CMP-00238-1	MPU-9250	1
U5	ISL29023IROZ-T7	SON65P210X75_HS-7N	CMP-00134-1	ISL29023IROZ-T7	1
U6	SHT21	SON100P300X110_HS-7N	CMP-00136-1	SHT21	1
U7	TMP006BIYZFR	YZF0008AHAH	CMP-0978-00003-2	TMP006BIYZFR	1
U8	BME280	BME280	CMP-00278-1	BME280	1
U9	PIC12LF1552-I/SN	M08A_N	CMP-00130-1	PIC12LF1552-I/SN	1
U10	TLV3701CDBVT	Z5+1_N	CMP-00131-1	TLV3701CDBVT	1
U11	RFM95W-868S2	RFM95W	CMP-00138-2		1
U13	TPS62736RGYR	RGY14-2050X2050TP	CMP-00239-2	TPS62736RGYR	1
X1, X2, X3, X4, X5, X6, X9, X10, X11, X12, X13, X14, X15, X16, X21, X22, X23	TX, RX, TEST, RST, VCC, GND, WU, DATA, SI, SCLK, SO, GND, VCC_ON, MCLR, Vcc, [No Value], Batt	TSW-150-07-G-S	CMP-00008-1	68001-101HLF	17
X18, X25, X27, X28	Vcc, Vcc_ON, Batt, Gnd	TSW-150-07-G-S	CMP-00008-2	68001-101HLF	4
Y1	ABS07-32.768KHz-T	ABRA-ABS07-2_V	CMP-0447-00001-2	ABS07-32.768KHZ-T	1
Y2	ABLS2-4.096MHZ-D4Y-T	ABRA-ABLS2-2_V	CMP-0277-00002-1	ABLS2-4.096MHZ-D4Y-T	1

ETH zürich

WuLoRa: Energy-Efficient IoT Sensor Node

Akos Pasztor
D-ITET, Semester Thesis
Spring Semester 2017

Supervisor:
Dr. Michele Magno

Professor:
Prof. Dr. Luca Benini

Introduction

Wireless Sensor Networks

- Purpose: sensing, data collection, logging, communication
- Long-range communication requires energy
- Critical Requirement:
  - Battery-life (low-power consumption, energy harvesting)

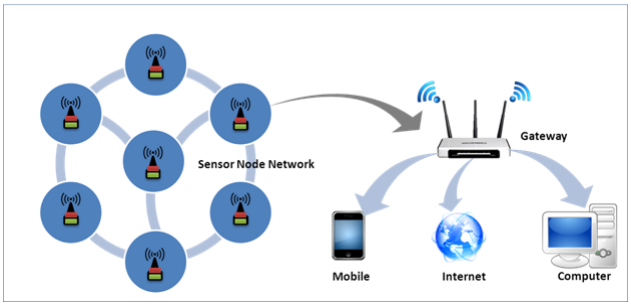

Introduction

Concept: Efficient IoT Node

- Battery-operated
- Energy Harvesting
- Sensing
- Communication
  - LoRa
  - Wake-Up Radio

Key Design Decisions

LoRa

- New modulation standard for IoT applications
- Enhanced for low power consumption
  - Rx: 10mW – 20mW
  - Tx: 400mW (+20dBm, to achieve max. distance)
- Uses 868MHz ISM band (in Europe)
- Long Range: 15km (5km in dense urban areas)
- Adaptive Data Rate (ADR)

Key Design Decisions

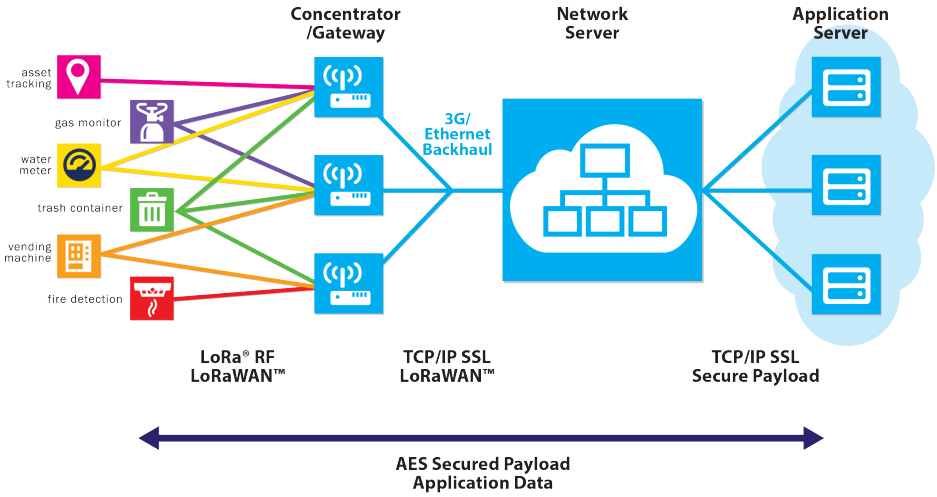

ETH zürich | Introduction | Design | Evaluation | Summary

Key Design Decisions

LoRa Nodes

- Class A (Avg. ~ 100uW)
  - Sleep → transmit
  - RX window only after transmission
  - Low energy, high latency (problem for safety-critical applications)
- Class B (Avg. ~ 1mW)
  - Ability to open extra RX slots
  - Requires scheduling
  - Moderate energy, moderate latency
- Class C (Avg. ~ 20mW)
  - Always-on listeners
  - High energy, low latency

Key Design Decisions

Latency Issue in Low-Power Applications

- Low-power applications → Class A LoRa devices
- Problem: latency vs. energy consumption (Rx: 10-20mW)
  - Problem with safety-critical applications
  - Idle listening → waste
  - Sleeping → high latency
- Promising idea: combine ultra-low power wake-up circuit with long-range transceivers
  - To achieve low-latency
  - Maintain low-power consumption
- What is a wake-up radio?

Key Design Decisions

Wake-Up Radio – developed at IIS

- Semi-active wake-up circuit with nanowatt consumption
  - 2µW consumption, -55dBm sensitivity
- Listens to the channel for OOK messages
- Issues an interrupt when a message is detected
- Address matching: ULP microcontroller

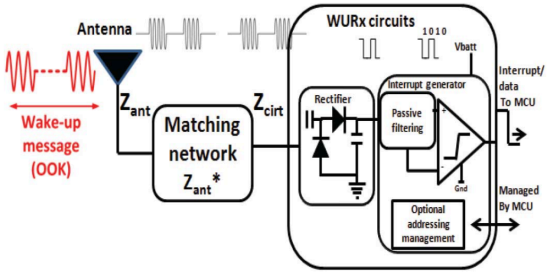

Clustered Network

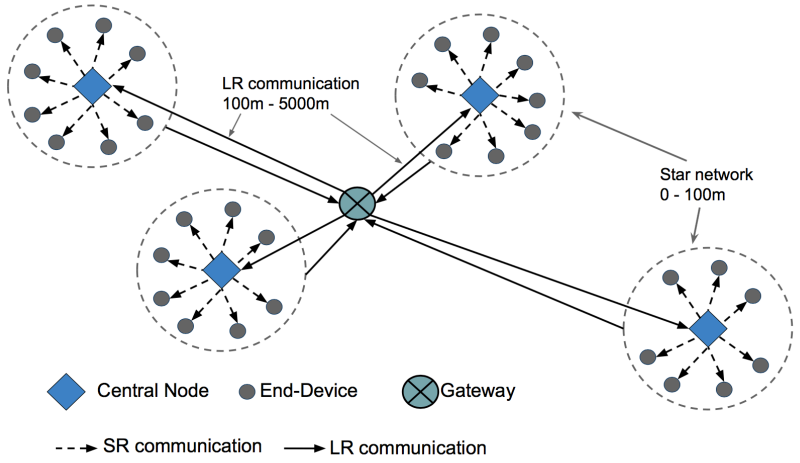

System Design

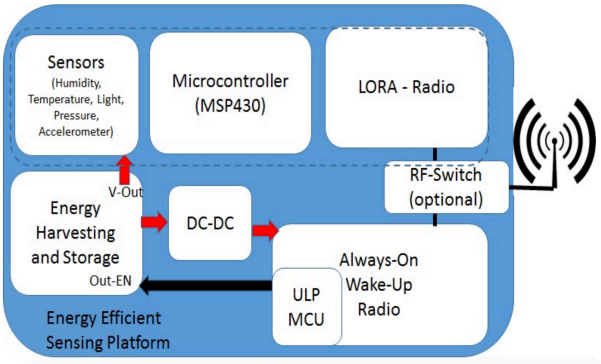

Features:

Dual MCU platform:

- MSP430 with FRAM
- PICLF1552 for WuR

LoRa radio:

- SX1276 from Semtech, featuring LoRa, OOK, …

Energy Harvesting:

- BQ25570 from TI
- Solar panel

Sensors:

- Temp & Humid. (SHT21)
- Barometric (BMP180)
- Infrared (TMP006)
- Light sensor (ISL29023)
- 9-axis IMU (MPU-9250)
- Battery gas gauge

Thesis Goals

- Debug preliminary prototype and correct the issues
  - Evaluate each subsystem
  - Test functionality
- Develop testing firmware for extensive analysis
- Perform power analysis for different scenarios
- Evaluate measurements
- Design new, improved prototype

System Design

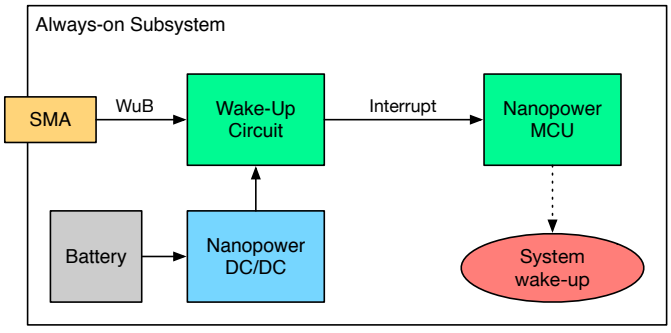

- -55dBm sensitivity
- TLV3701 Comparator
  - 560nA supply current
- PIC12LF1552
  - 20nA in standby mode
- TPS62736 nano-power buck
  - > 90% efficiency even at low current draws

System Design

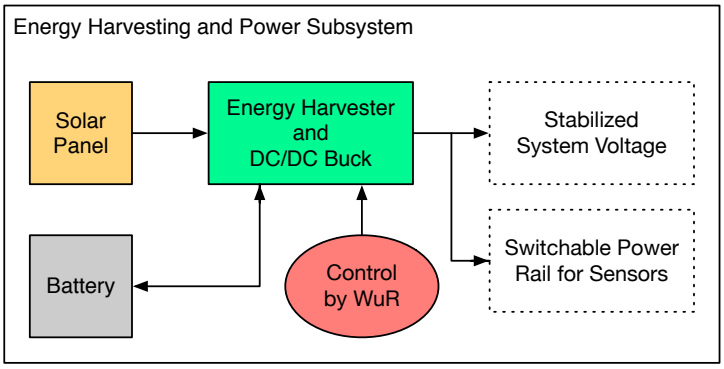

- Solar panel
- TI BQ25570
  - 90% efficiency, Energy harvesting from 100mV, < 200nA quiescent current
- Wake-up radio can disable the entire power system to achieve lowest power consumption

System Design

- Subsystems required careful design:
- Using multiple voltage rails can introduce the following issue:
- Inter-subsystem leakage through pin protection

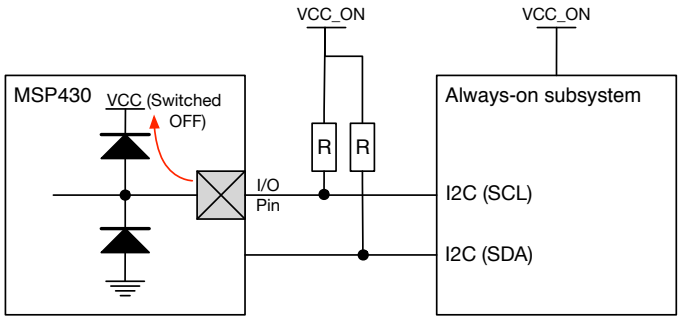

System Design

Power subsystem issues

- Energy Harvester IC
  - Output voltage and threshold voltages
  - Buck-disabling circuit is problematic: boost output can only enable the buck
- Sensor and radio power rail was redesigned:
  - They are supplied directly from the main power rail
  - Main power rail is switched on/off by the wake-up radio

System Design

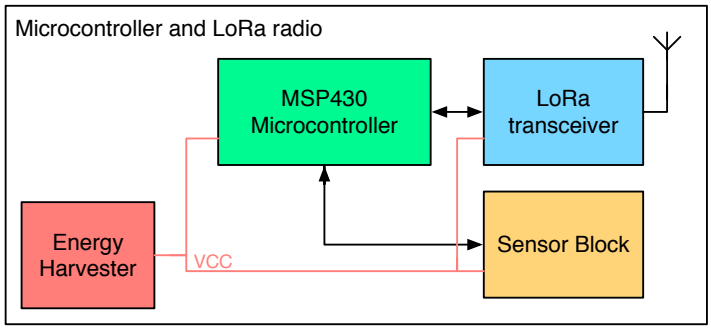

- TI MSP430 with FRAM
- Semtech SX1276
  - -148dBm sensitivity
  - 20dBm TX power
  - Multiple modulations

System Design

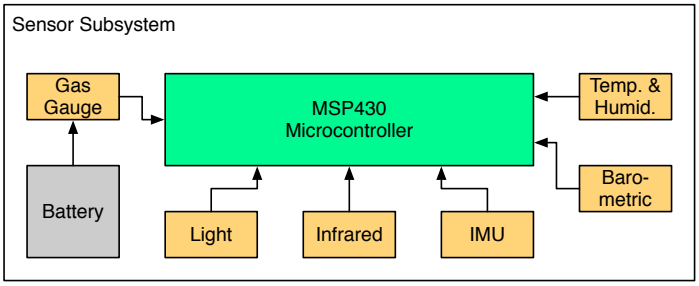

- Temp & Humid. (SHT21) ~ 1µW (idle) | 1mW (meas.)
- Barometric sensor (BMP180) ~ 10µW (idle) | 2mW (meas.)
- Infrared sensor (TMP006) ~ 3µW (idle) | 0.7mW (meas.)
- Light sensor (ISL29023) ~ 1µW (idle) | 0.3mW (meas.)
- 9-axis IMU (MPU-9250) ~ 20µW (idle) | 9mW (meas.)
- Battery gas gauge ~ 3µW (idle) | 0.3mW (meas.)

System Design

Sensor subsystem issues

- IMU
  - Wrongly connected and routed
  - Communication lines were switched up
- Battery fuel gauge
  - Wrongly connected
  - Confusing jumper system
  - Wrongly connected jumpers can cause damage (short between VCC and BAT+)

System Design

New prototype

- Detailed ECO
- New schematics
  - Redrawn critical circuits
  - Hierarchical design
  - Additional GPIO header
- PCB Layout
  - Size and dimensions are kept the same
  - Design improvements for stability, and noise resilience
    - Polygon pour optimization (Antenna-effect, GND-drift)
    - New jumper system
    - Better labelling

New Prototype Design

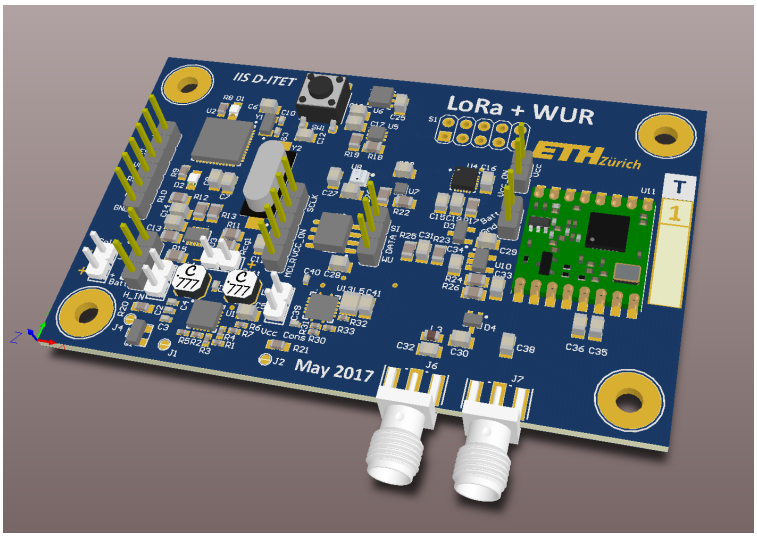

Experimental Results

Extensive Power Analysis

- RocketLogger
- Various scenarios and parameters

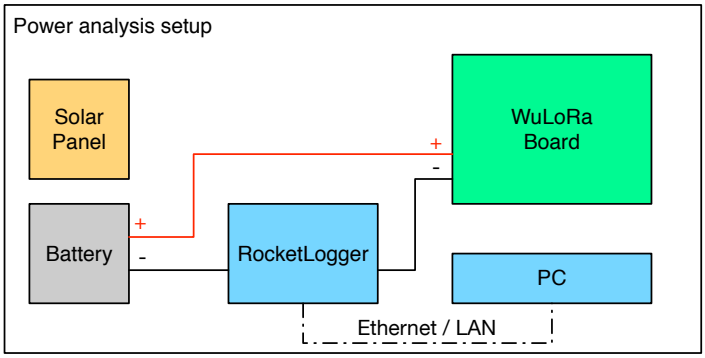

Experimental Results

Power Analysis Scenarios

1. Always-on subsystem, PIC is sleeping.
2. Always-on subsystem, PIC is active.
3. MSP430 is active. Sensors, radio are off.
4. Sensor measurements, radio is off (powered on but stayed in shutdown mode)
5. Radio is in OOK mode, +10dBm TX power
6. Radio is in LoRa mode
   - Tx: 0dBm, +5dBm, +10dBm, +14dBm, +17dBm, +20dBm
   - Fixed data rate

Experimental Results

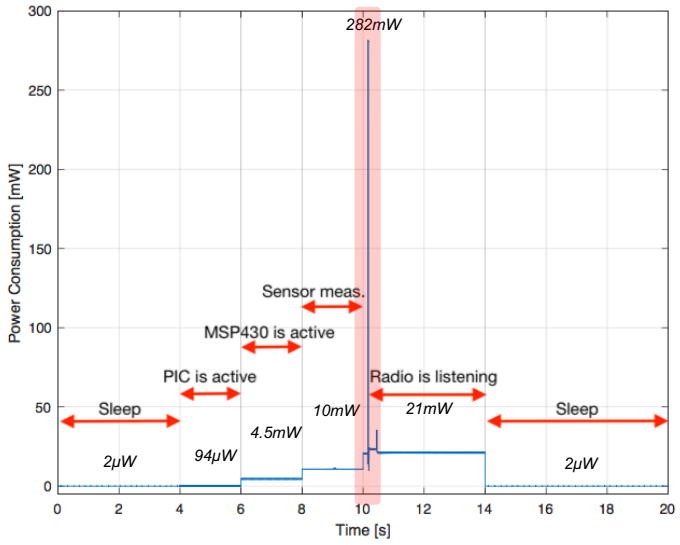

System voltage:
- 3.0 V

LoRa parameters:
- DR: 12
- +10dBm (TX)

Experimental Results

Power Analysis Results

Time	Event	Power Dissipation
$0s - 4s$	System sleep (WuR is listening)	$2.091\mu W$
$4s - 6s$	PIC is active, rest of the system is in sleep	$93.830\mu W$
$6s - 8s$	MSP430 and main power subsystem is active	$4.534mW$
$8s - 10s$	Sensor measurement	$10.671mW$
$10s$	Radio is switched on (LoRa with $+10dBm$ TX power) and sends packet	$282mW$
$10s - 14s$	Radio is listening	$21.011mW$
$14s - 20s$	System sleep	$2.091\mu W$

Table 4.1: Results of power analysis

Experimental Results

Power Analysis Results

- Battery estimation
  - Without harvester
  - 1 WuB in every hour: Sensor measurements, LoRa transmission
  - 800mAh battery

ETH zürich | Introduction | Design | Evaluation | Summary

Experimental Results

Power Analysis Results

- Battery estimation
  - Without harvester
  - 1 WuB in every hour: Sensor measurements, LoRa transmission
  - 800mAh battery

- Five and a half years of continuous operation!
  - Low-power consumption was maintained
  - Communication latency was reduced with the help of the wake-up radio

Summary

Future work

- Further improve each subsystem
- Evaluate new SoC-s designed for IoT applications
  - ARM Cortex M0+ with SX1276 by Murata
  - ST's L-series Cortex-core MCU-s are leaders in ULP applications
  - Eliminates the need of WUR microcontroller
  - Reduces size, complexity
  - Better optimization

ETH zürich | Introduction | Design | Evaluation | Summary

Summary

Conclusion

- ✓ Evaluate each subsystem on preliminary hardware
- ✓ Debug preliminary prototype and correct the issues
- ✓ Develop testing software for extensive analysis
- ✓ Perform power analysis for different scenarios
- ✓ Evaluate measurements
- ✓ Design new, improved prototype

ETH

Eidgenössische Technische Hochschule Zürich
Swiss Federal Institute of Technology Zurich

Declaration of originality

The signed declaration of originality is a component of every semester paper, Bachelor's thesis, Master's thesis and any other degree paper undertaken during the course of studies, including the respective electronic versions.

Lecturers may also require a declaration of originality for other written papers compiled for their courses.

I hereby confirm that I am the sole author of the written work here enclosed and that I have compiled it in my own words. Parts excepted are corrections of form and content by the supervisor.

Title of work (in block letters):

WuLoRa: Energy-Efficient IoT Sensor Node

Authored by (in block letters):
For papers written by groups the names of all authors are required.

Name(s):	**First name(s):**
Pasztor	Akos

With my signature I confirm that

- I have committed none of the forms of plagiarism described in the 'Citation etiquette' information sheet.
- I have documented all methods, data and processes truthfully.
- I have not manipulated any data.
- I have mentioned all persons who were significant facilitators of the work.

I am aware that the work may be screened electronically for plagiarism.

Place, date

Zürich, 19.06.2017

Signature(s)

For papers written by groups the names of all authors are required. Their signatures collectively guarantee the entire content of the written paper.